Periodic Hamiltonian systems in shape optimization problems with Neumann boundary conditions

Cornel Marius Murea[a,*], Dan Tiba[b]

[a] *Département de Mathématiques,*
Institut de Recherche en Informatique, Mathématiques, Automatique et Signal,
Université de Haute Alsace, France
[b] *Institute of Mathematics (Romanian Academy), Bucharest, Romania*

Abstract

The recent implicit parametrization theorem, based on simple Hamiltonian systems, allows the description of domains and their boundaries and, consequently, it provides a general fixed domain approximation method in shape optimization problems, using optimal control theory. Here, we discuss topology and shape optimization in the difficult case of Neumann boundary conditions, with a combined cost including both distributed and boundary observation. We give an unexpected general equivalence property with constrained optimal control problems, preserving differentiability. An important new ingredient in the arguments is the differentiability of the period for the Hamiltonian systems, with respect to functional variations. Due to the differentiability properties, we can use descent algorithms of gradient type. In the experiments, our approach can modify the topology both by closing holes or by creating new holes. We underline the applicability of this new methodology to large classes of shape optimization problems.

Keywords: Hamiltonian systems, implicit parametrizations, topology optimization, optimal control, Neumann boundary conditions, boundary and topological variations
2020 MSC: 49J50, 49M20, 49Q10

*Corresponding author
Email addresses: `cornel.murea@uha.fr` (Cornel Marius Murea), `dan.tiba@imar.ro` (Dan Tiba)

1. Introduction

Shape optimization has started its development especially in the last quarter of the previous century and we just quote several monographs devoted to this subject Pironneau [39], Haslinger and Neittaanmäki [22], Sokolowski and Zolesio [43], Delfour and Zolesio [17], Neittaanmäki, Sprekels and Tiba [33], Bucur and Buttazzo [11], Henrot and Pierre [25], where more details on the history of the subject and comprehensive references can be found. Concerning topology optimization, several approaches like homogenization and the material distribution method, [1], [9], the level-set method [4], [1], [2], topological asymptotics and the topological gradient [6], [35], [36] have been intensively investigated. We also mention the recent developments [5], [18] devoted to the study of the topological gradient in the case of the quasilinear elliptic equations. The literature in these respects is very rich and we have indicated just a brief selection. Each of these techniques has known advantages and/or drawbacks and a "complete" solution is still to be found.

A typical example of shape optimization problem, defined on a given family of domains $\Omega \in \mathcal{O}$, $\Omega \subset D$ a prescribed holdall bounded domain, has the following structure:

$$\min_{\Omega \in \mathcal{O}} \int_\Lambda j\left(\mathbf{x}, y_\Omega(\mathbf{x})\right) d\mathbf{x}, \tag{1.1}$$

$$A\, y_\Omega = f \text{ in } \Omega, \tag{1.2}$$

$$B\, y_\Omega = 0 \text{ on } \partial\Omega \tag{1.3}$$

where Λ may be Ω or some fixed given subdomain $E \subset \Omega$, or $\partial\Omega$ or some part of it; and B is some boundary operator expressing the boundary condition, A is some (elliptic) differential operator, $f \in L^p(D)$, $p > 2$ given, and $j(\cdot,\cdot)$ is a Carathéodory function. The solution $y_\Omega \in W^{2,p}(\Omega) \subset C^1(\overline{\Omega})$ has here maximal elliptic regularity and the used formulas (including derivatives) have a clear pointwise meaning, in the sequel. In principle, it is possible to work with $p = 2$ as well, by means of the trace theorem on $\partial\Omega$, but one of our aims is to avoid the references to the unknown geometry and to develop a purely analytic framework, see (3.1). More constraints on the unknown domains Ω, or on the state y_Ω, more general cost functionals may be taken into account. Regularity assumptions on $\Omega \in \mathcal{O}$, on $j(\cdot,\cdot)$, other hypotheses, will be imposed as necessity appears.

Many geometric optimization problems arise in mechanics: minimize the thickness, the volume, the stresses, etc., in a plate, a beam, a curved rod in dimension three, an arch, a shell. Due to the formulation of the mechanical models, the geometric characteristics of the object (thickness, curvature) enter as coefficients in the governing differential system. Consequently, such geometric optimization problems take the form of an optimal control problem in a given domain, with the control acting in the coefficients. See [8], [7], [33] Ch VI, where detailed presentations, including numerical examples, may be found.

In fact, general shape optimization problems (1.1)-(1.3) have a similar structure with optimal control problems, the difference being that the minimization parameter is the unknown geometry itself, $\Omega \in \mathcal{O}$. It is a natural question to find a method that reduces/approximates general optimal design problems to/via optimal control theory, and some examples already appear in the classical monograph of Pironneau [39]. In the case of Dirichlet boundary conditions, several approaches have been developed [32], [31], [29], [30] allowing both shape and topology optimization, but no other boundary conditions. Essential ingredients are functional variations that combine both boundary and topology changes, and the recent implicit parametrization method based on the representation of the geometry via iterated Hamiltonian systems [45], [34], [46], [47]. We present here a general approach, enjoying differentiability and equivalence with constrained control problems and we show that it also works in the difficult case of Neumann boundary conditions, where the usual zero extension technique from the Dirichlet case, cannot be applied. The approach from this paper may be also employed for the Robin boundary conditions, for certain nonlinear boundary conditions or nonlinear equations, etc., but we do not examine now such questions since any of them requires a detailed new investigation. Moreover, we stress that there are already results in this respect, in the literature, (for instance, in the monographs [35], [36]), by using various shape optimization or topology optimization techniques. Our method combines both aspects in a natural way and gives new information from the theoretical and the computational points of view.

The methodology is of fixed domain type and it has important advantages at the numerical level: it avoids remeshing and recomputing the mass matrix in each iteration of the algorithm. Related ideas are also applicable in free boundary problems, see [50], [20], [21], or in optimization and control, [48].

Concerning topological variations, we underline that the well known level set method [37], [38], [1], [28] is essentially different from our approach. In our method, while we also use level functions, no Hamilton-Jacobi equation is needed and simple ordinary differential Hamiltonian systems can handle the unknown geometry and its variations (of general functional type). We work in dimension two, $D \subset \mathbb{R}^2$, since the important periodicity argument is based on the Poincaré-Bendixson theorem [26], [40], and certain related developments. We obtain in this way a global parametrization of the boundary of the unknown domains and this is an essential point. Extending to higher dimension would require extending this global parametrization/representation, which seems a difficult task. In dimension three, in [34], in one example involving the torus, it is shown that the representation is not global although both (iterated) Hamiltonian systems used there have periodic solutions. Dimension two is a case of interest in shape optimization. Moreover, our method is also different from the well known topological asymptotics and it allows the computation of the gradient and the use of gradient descent methods in the numerical experiments. In fact, we employ here a derivative with respect to the geometry that takes into account simultaneously both boundary and topological variations in a natural way (the type of geometric perturbation is not prescribed, but automatically chosen during the iterative process). For topological asymptotics, we quote the papers by Amstutz [3], Masmoudi and his co-authors [23], the monographs of Sokolowski and his collaborators [35], [36], and their references.

Another topology optimization method, also based on optimal control theory, was developed in [27], [15], [16], in the case of multi-material optimal distribution problems.

Comparing with our previous works [47], [29], both are dealing just with Dirichlet conditions and distributed cost. The first one includes an equivalence property of a different type and without differentiability, that makes applications difficult. The second one investigates just the approximation question, has strong hypotheses (not necessary here) and the differentiability properties have a partial character. A simplified adjoint system is used and ad-hoc partial descent directions are put into evidence (i.e. with respect just to some terms of the cost functional), without a complete justification of the algorithm. In contrast, in the present work, we indicate the mathematical justification of our solution technique and of the resulting methodology.

The paper is organized as follows. In the next Section, we collect some preliminaries and we give the precise formulation of the problem. Both distributed and boundary observations are taken into account. In Section 3, we introduce the fixed domain approximation process as an optimal control problem, we prove the equivalence between the two types of problems and a general approximation property is obtained under very weak conditions, and we also obtain some error estimates. As another corollary of the employed methods, an existence result is proved as well. Section 4 is devoted to the differentiability properties of our approach, that give the basis for numerical algorithms of gradient type. A key technical development is the proof of the differentiability of the period in Hamiltonian systems, with respect to functional variations and this allows the introduction of a novel adjoint system. A theoretical analysis of the discretization process, including the computation of the cost gradient, together with numerical examples are discussed in the last two Sections. At the computational level, we use gradient algorithms and the topology can be modified either by closing or by opening holes. The examples are of academic type and put into evidence some variants of our approaches and their properties: descent, approximation, topological and boundary changes, etc. This methodology has a purely analytic character and can be applied to many geometric optimization problems, with respect to the considered boundary conditions and to the differential operators. The lack of convexity (see Ex. 1, b in the last section, that admits an infinity of global solutions) makes it very difficult to handle numerically examples with topological changes. Even if the global minimum is known and the optimal domain has holes, the algorithm may stop in a local minimum close to the initial guess, without changing the topology.

To summarize, we consider as advantages of our approach the fact that it is relevant both at the theoretical level and at the computational level, the possible applicability of our optimal control technique to a large class of state systems and boundary conditions, the possibility to work with general cost functionals (for instance, boundary observation is also considered in this paper), the fact that we can compute the gradient of the cost via a novel adjoint system and we use gradient methods in the optimization process, the fact that we use simple Hamiltonian systems instead of Hamilton-Jacobi equations. We also obtain a new equivalence result between topology optimization and a class of constrained control problems. While, in this article, we stress approximation properties, we intend as well to apply the equivalence and the new adjoint system for the examination of the optimality conditions, in a future work.

As drawbacks, we mention the regularity hypotheses and the fact that our study is valid just in dimension two. Both are mainly due to the (essential) use of the Poincaré - Bendixson theory that allows a global representation of the unknown boundary via Hamiltonian parametrizations. We also underline that computing boundary observation for Neumann conditions, naturally requires regularity properties both for the unknown geometry and for the state unknown.

2. Problem formulation and preliminaries

Let $\mathcal{O}$ be a given family of open, connected sets, $\Omega \subset D$, not necessarily simply connected, where $D \subset \mathbb{R}^2$ is a holdall bounded domain and Ω, D have both $\mathcal{C}^{1,1}$ boundaries.

In each $\Omega \in \mathcal{O}$, we consider the Neumann boundary value problem

$$-\Delta y_\Omega + y_\Omega = f \text{ in } \Omega, \tag{2.1}$$
$$\frac{\partial y_\Omega}{\partial \mathbf{n}} = \alpha \text{ on } \partial\Omega, \tag{2.2}$$

where $f \in L^p(D)$, $\alpha \in W^{1,p}(D)$, $p > 2$ are given. It is known that (2.1), (2.2) has a unique solution $y_\Omega \in W^{2,p}(\Omega)$, more general elliptic operators may be taken into account in (2.1) (or even evolution operators, see [49]), the regularity conditions on the boundary may be relaxed, Grisvard [19]. Here, it is important to work in $\mathbb{R}^2$ since Poincaré-Bendixson type arguments are essential in the proof of the global existence result for the Hamiltonian system (2.10)-(2.12), introduced in the sequel for the description of the unknown geometries. In fact, all the other arguments to be used in this work are valid in arbitrary dimension, where iterated Hamiltonian systems are necessary for the description of the geometry, but their solution is just local [46].

We associate to the system (2.1), (2.2) a cost functional that combines distributed and boundary observation (the necessary regularity conditions are detailed in the sequel):

$$\min_{\Omega \in \mathcal{O}} \left\{ \int_E J\left(\mathbf{x}, y_\Omega(\mathbf{x})\right) d\mathbf{x} + \int_\Omega L\left(\mathbf{x}, y_\Omega(\mathbf{x})\right) d\mathbf{x} + \int_{\partial\Omega} j\left(\mathbf{x}, y_\Omega(\mathbf{x})\right) d\sigma \right\}, \tag{2.3}$$

where $E \subset\subset D$ is a given subdomain such that $E \subset \Omega$ for any $\Omega \in \mathcal{O}$ and $J(\cdot,\cdot)$, $L(\cdot,\cdot)$, $j(\cdot,\cdot)$ are Carathéodory functions. More constraints (for instance, on the state y_Ω) may be added to the shape optimization problem (2.1)-(2.3), denoted by $(\mathcal{P})$. Such state constraints may be approached with techniques from control theory, in the setting of the optimal control methodology that we use here. However, considerable supplementary difficulties may arise and we don't discuss this possible extension now. The precise assumptions will be formulated as necessity appears. The presence of cost integral functionals defined on both E, Ω may look redundant. We underline that the domain E corresponds to certain requirements specific to many examples (the unknown domains should contain a given region, the unknown state should be close to some prescribed values there, etc.). This term may also include standard tracking type cost functionals. The example $L(\cdot,\cdot) = 1$, corresponding to $meas(\Omega)$, shows that the second term in the cost may be interpreted as measuring the "size" of the geometric control; it also may include tracking type functionals.

The approach based on functional variations [31], [32], [47] assumes that the family of admissible domains $\mathcal{O}$ is obtained starting from a family $\mathcal{F} \subset \mathcal{C}(\overline{D})$ of level functions via the relation:

$$\Omega = \Omega_g = int\left\{\mathbf{x} \in D;\ g(\mathbf{x}) \leq 0\right\}, \quad g \in \mathcal{F}. \tag{2.4}$$

While Ω_g defined in (2.4) is an open set and may have many connected components, the domain Ω_g that we use in the sequel is the component that contains E. This is possible if we assume

$$g(\mathbf{x}) \leq 0, \quad \forall \mathbf{x} \in E, \quad \forall g \in \mathcal{F}. \tag{2.5}$$

Another variant, that may be used in the definition of the domain Ω_g, is to assume

$$\mathbf{x}_0 \in \partial\Omega_g, \quad \forall g \in \mathcal{F} \tag{2.6}$$

for some $\mathbf{x}_0 \in D \setminus \overline{E}$, given. Here, one has to impose on the family $\mathcal{F}$ the simple constraint

$$g(\mathbf{x}_0) = 0, \quad \forall g \in \mathcal{F}. \tag{2.7}$$

In this context, it is important to consider the closed bounded set:

$$G_g = \{\mathbf{x} \in D;\ g(\mathbf{x}) = 0\} \tag{2.8}$$

associated to any $g \in \mathcal{F}$. If $\mathcal{F} \subset \mathcal{C}(\overline{D})$ without further conditions, then $meas(G_g) > 0$ is possible. To avoid this, we further assume in the sequel, see [47], that $\mathcal{F} \subset \mathcal{C}^1(\overline{D})$ and

$$|\nabla g(\mathbf{x})| > 0, \quad \forall \mathbf{x} \in G_g, \quad \forall g \in \mathcal{F}. \tag{2.9}$$

Then, by (2.6)-(2.9) and the implicit functions theorem, we get $G_g = \partial\Omega_g$ is of class $\mathcal{C}^1$, $\Omega_g = \{\mathbf{x} \in D;\ g(\mathbf{x}) < 0\}$ and the Hamiltonian system

$$\begin{aligned} z_1'(t) &= -\frac{\partial g}{\partial x_2}\left(z_1(t), z_2(t)\right), \quad t \in I_g, && (2.10)\\ z_2'(t) &= \frac{\partial g}{\partial x_1}\left(z_1(t), z_2(t)\right), \quad t \in I_g, && (2.11)\\ (z_1(0), z_2(0)) &= \mathbf{x}_0 \in \partial\Omega_g, && (2.12) \end{aligned}$$

where I_g is the local existence interval for (2.10)-(2.12) with solution $[z_1, z_2] \in C^1(I_g)$, gives a local parametrization of $\partial\Omega_g$ around $\mathbf{x}_0$, [45]. The solution is unique due to the Hamiltonian structure [46], although the right-hand side is just continuous. We also assume that

$$g(\mathbf{x}) > 0, \quad \forall \mathbf{x} \in \partial D, \quad \forall g \in \mathcal{F} \tag{2.13}$$

which ensures that $G_g \cap \partial D = \emptyset$ for $g \in \mathcal{F}$. The choice of $g \in \mathcal{F}$ in the definition of the domain Ω_g via (2.4), (2.5) or (2.6) is not unique. It may be chosen positive in $D \setminus \Omega_g$.

Notice that the family $\mathcal{O}$ of $\mathcal{C}^1$ domains defined by (2.4), (2.5) or (2.6) is rich, they may be multiply connected and this is one reason why this approach combines boundary and topological variations in shape optimization.

Moreover, under hypothesis (2.9), more regularity can be obtained for $\partial\Omega_g$ if more regularity is imposed on $\mathcal{F}$. This ensures the previously mentioned regularity properties for the solution of (2.1), (2.2). The cost (2.3) and its approximation (in the next section), are well defined. Condition (2.9) plays, in fact, an essential role in the Poincaré-Bendixson theory, [26], [40], applied to (2.10)-(2.12).

It is proved in [47], that the hypotheses (2.9) and (2.13) are sufficient for the global existence in (2.10)-(2.12):

Theorem 2.1. *For any $\mathbf{x}_0 \in D \setminus \overline{E}$, with $g(\mathbf{x}_0) = 0$, the solution of (2.10)-(2.12) is periodic and I_g may be chosen as its period, $I_g = [0, T_g]$.*

Namely, the limit cycle situation from the Poincaré-Bendixson theory is not possible here. If $\partial\Omega_g$ is not connected, its complete description may be obtained via (2.10)-(2.12), by choosing an initial condition on each component. Another useful property proved in [47] is

Theorem 2.2. *Under hypotheses (2.9) and (2.13), the compact set G_g has a finite number of connected components, for any given $g \in \mathcal{F}$.*

Clearly, the number of the connected components may be unbounded over the whole family $\mathcal{F}$.

3. Approximation and equivalence

One idea behind our approach is to penalize the boundary condition on the unknown domains. We extend the state equation (2.1) from Ω_g to D by adding a distributed control term in the right-hand side and the boundary condition (2.2) is approximated in the cost by a quadratic term defined on $\partial\Omega_g$. These computations are possible due to the Hamiltonian representation of the unknown geometries, Thm. 2.1 and Thm. 2.2. In this way, we obtain a new penalization/regularization approach that has good differentiability properties and is formulated as an optimal control problem with two independent controls $g \in \mathcal{F}$ and u measurable, satisfying certain conditions. Unexpectedly, we also show that the corresponding constrained optimal control problem is even equivalent with the shape optimization problem, in general situations. The penalization of the last term in (3.1) is motivated by the equivalence result Corollary 3.1 and standard optimization techniques to remove the constraint. Notice that we introduce no approximation in the new state equation, it is just an extension operation that preserves differentiability properties. In case the state system would be perturbed by a corresponding penalization quantity, the approximation properties would be valid just for the state system, while the properties of the corresponding optimization problems are difficult to infer, see the survey [31] or [30]. We also regularize the second term in the original cost (2.3) and we get the control problem:

$$\min_{g,u}\left\{\int_E J(\mathbf{x},y(\mathbf{x}))\,d\mathbf{x}+\int_D[1-H^\epsilon(g(\mathbf{x}))]L(\mathbf{x},y(\mathbf{x}))\,d\mathbf{x}\right. \tag{3.1}$$
$$+\int_{I_g} j(\mathbf{z}(t),y(\mathbf{z}(t)))\,|\mathbf{z}'(t)|dt$$
$$\left.+\frac{1}{\epsilon}\int_{I_g}\left[\nabla y(\mathbf{z}(t))\cdot\frac{\nabla g(\mathbf{z}(t))}{|\nabla g(\mathbf{z}(t))|}-\alpha(\mathbf{z}(t))\right]^2|\mathbf{z}'(t)|dt\right\}$$

subject to

$$-\Delta y+y = f+g_+^2u, \quad \text{in } D, \tag{3.2}$$
$$y = 0, \quad \text{on } \partial D, \tag{3.3}$$

and (2.5). Above, $\epsilon>0$, $H^\epsilon(\cdot)$ is a regularization of the Heaviside function, g_+ is the positive part of g and we assume $g>0$ outside Ω_g, $\mathbf{z}(t)=(z_1(t),z_2(t))$ is the solution of (2.10)-(2.12), the state $y\in W^{2,p}(D)\cap H_0^1(D)$ from (3.2), (3.3) depends on $g\in\mathcal{F}$ and u is measurable such that $g_+^2u\in L^p(D)$, $p>2$. Clearly, $1-H(g)$ is the characteristic function of Ω_g and $1-H^\epsilon(g)$ is its regularization, that is $H^\epsilon(r)\to H(r)$ for $r\in\mathbb{R}$ and $H^\epsilon(\cdot)$ is at least in $\mathcal{C}^1(\mathbb{R})$ and with values in $[0,1]$. In dimension 2, we have $y\in\mathcal{C}^1(\overline{D})$ by the Sobolev theorem and all the terms in (3.1) make sense. The penalization term in (3.1) includes a computable formula (depending just on g and u) for

$$\int_{\partial\Omega_g}\left|\frac{\partial y}{\partial\mathbf{n}}(s)-\alpha(s)\right|^2 ds$$

based on the Hamiltonian representation (2.10)-(2.12) of $\partial\Omega_g$ and the fact that the unit normal to $\partial\Omega_g=G_g$ is given by $\frac{\nabla g(z_1(t),z_2(t))}{|\nabla g(z_1(t),z_2(t))|}$ in $(z_1(t),z_2(t))\in\partial\Omega_g$ and it is well defined due to (2.9). A similar interpretation is valid for the third term in (3.1) and the problem (3.1)-(3.3) can be interpreted itself as a shape optimization problem in D, with constraint (2.5) on g. In case $\partial\Omega_g$ has several connected components (their number depends on g and is finite by Thm. 2.2), then the penalization term has to be replaced by a finite sum of similar terms associated to each component of $\partial\Omega_g$, by fixing some initial condition in

(2.10)-(2.12) on each component of $\partial\Omega_g$. In the numerical examples, we limit this number from above by some constant in all the iterations, but the actual number of components of $\partial\Omega_g$ may still vary from one iteration to the other and similarly for the number of the penalization terms in the cost. This has a simple computational implementation since all such penalization terms are similar, just the component of $\partial\Omega_g$ is different. It is to be noticed that, in the "extended" equation (3.2), (3.3), we have Dirichlet boundary conditions, while the original state system (2.1), (2.2) is a Neumann boundary value problem. It turns out that the approximation and the equivalence properties of (3.1)-(3.3) remain valid even with this change of boundary conditions and we want to stress this property. In fact, it is also easier to work with (3.3) in the finite element discretization, in the next sections.

Proposition 3.1. *Let $J(\cdot,\cdot)$, $L(\cdot,\cdot)$ and $j(\cdot,\cdot)$ be Carathéodory functions on $D\times\mathbb{R}$, J bounded from below by a constant and L, j positive. Let $\mathcal{F}\subset\mathcal{C}^2(\overline{D})$ satisfy (2.9), (2.13) and denote by $[y_n^\epsilon, g_n^\epsilon, u_n^\epsilon]$ a minimizing sequence in the penalized problem (3.1)-(3.3), (2.5). Then, on a subsequence denoted by $n(m)$, the cost associated to the pairs $[\Omega_{g^\epsilon_{n(m)}}, y^\epsilon_{n(m)}]$ in (2.3) approaches some value majorized from above by $\inf(\mathcal{P})$, (2.1) is satisfied by the pairs $[\Omega_{g^\epsilon_{n(m)}}, y^\epsilon_{n(m)}]$ and (2.2) is valid with a perturbation of order $\epsilon^{1/2}$.*

Since the boundary condition (2.2) may be violated, the pairs $[\Omega_{g^\epsilon_{n(m)}}, y^\epsilon_{n(m)}]$ are not necessarily admissible for the shape optimization problem (2.1)- (2.3). This will be clarified in Proposition 3.2, via an error estimate independent of the geometry.

Proof. The proof follows ideas from [47], [29]. Let $[y_{g_m}, g_m]\in W^{2,p}(\Omega_{g_m})\times\mathcal{F}$ be a minimizing sequence for the problem (2.1)-(2.5). Here, $\partial\Omega_{g_m}$ is $\mathcal{C}^2$ and this ensures the regularity $y_{g_m}\in W^{2,p}(\Omega_{g_m})$ due to $f\in L^p(D)$. There is $\widetilde{y}_{g_m}\in W^{2,p}(D\setminus\overline{\Omega}_{g_m})$, not unique, such that $\widetilde{y}_{g_m}=y_{g_m}$ on $\partial\Omega_{g_m}$, $\frac{\partial\widetilde{y}_{g_m}}{\partial\mathbf{n}}=\frac{\partial y_{g_m}}{\partial\mathbf{n}}=0$ on $\partial\Omega_{g_m}$, $\widetilde{y}_{g_m}=0$ on ∂D. We define an admissible control in (3.2) by

$$u_{g_m}=-\frac{\Delta\widetilde{y}_{g_m}+f-\widetilde{y}_{g_m}}{(g_m)_+^2},\quad \text{in } D\setminus\overline{\Omega}_{g_m}, \tag{3.4}$$

and zero otherwise. We infer by (3.4) that $(g_m)_+^2 u_{g_m}$ is in $L^p(D)$ and g_m, u_{g_m} is an admissible control pair for the penalized problem (3.1)-(3.3), (2.5). Moreover, the corresponding state in (3.2), denoted by y_m, is obtained by concatenation of y_{g_m} and $\widetilde{y}_{g_m}$ and the corresponding penalization term in (3.1) is null. This construction is also valid in the case Ω_{g_m} is not simply connected. The corresponding cost in (3.1) is majorized by the one in (2.3) if we choose $H^\epsilon(\mu) = 1$ for $\mu > 0$.

Due to the above argument and to the following explanation below, we obtain

$$
\begin{aligned}
& \int_E J\left(\mathbf{x}, y^\epsilon_{n(m)}(\mathbf{x})\right) d\mathbf{x} + \int_D [1 - H^\epsilon(g^\epsilon_{n(m)})] L\left(\mathbf{x}, y^\epsilon_{n(m)}(\mathbf{x})\right) d\mathbf{x} \\
& + \int_{I_{g^\epsilon_{n(m)}}} j\left(\mathbf{z}^\epsilon_{n(m)}(t), y^\epsilon_{n(m)}(\mathbf{z}^\epsilon_{n(m)}(t))\right) |\mathbf{z}^{\epsilon\prime}_{n(m)}(t)| dt \\
& + \frac{1}{\epsilon} \int_{I_{g^\epsilon_{n(m)}}} \left[\nabla y^\epsilon_{n(m)}(\mathbf{z}^\epsilon_{n(m)}(t)) \cdot \frac{\nabla g^\epsilon_{n(m)}(\mathbf{z}^\epsilon_{n(m)}(t))}{|\nabla g^\epsilon_{n(m)}(\mathbf{z}^\epsilon_{n(m)}(t))|} - \alpha(\mathbf{z}^\epsilon_{n(m)}(t))\right]^2 \\
& \times |\mathbf{z}^{\epsilon\prime}_{n(m)}(t)| dt \\
\leq \; & \int_E J\left(\mathbf{x}, y_m(\mathbf{x})\right) d\mathbf{x} + \int_{\Omega_{g_m}} L\left(\mathbf{x}, y_m(\mathbf{x})\right) d\mathbf{x} + \int_{\partial\Omega_{g_m}} j\left(\mathbf{x}, y_m(\mathbf{x})\right) d\sigma \\
\to \; & \inf(\mathcal{P})
\end{aligned} \tag{3.5}
$$

for $m \to \infty$. In (3.5), the index $n(m)$ is big enough in order to have the left-hand side in (3.5) smaller than the cost (3.1) associated to the admissible triple $[g_m, u_{g_m}, y_m]$. Moreover, $\mathbf{z}^\epsilon_{n(m)}$ is the solution of (2.10)-(2.12) associated to $g^\epsilon_{n(m)}$.

Since $J(\cdot,\cdot)$, $L(\cdot,\cdot)$ and $j(\cdot,\cdot)$ are appropriately bounded from below, from (3.5), we get the boundedness of the penalization term on the subsequence $n(m)$. This yields the last statement of Proposition 3.1, on $\partial\Omega_{g^\epsilon_{n(m)}}$. As $\left(g^\epsilon_{n(m)}\right)_+$ is null in $\Omega_{g^\epsilon_{n(m)}}$, we see that (2.1) is satisfied in $\Omega_{g^\epsilon_{n(m)}}$, due to (3.2). The evaluation by $\inf(\mathcal{P})$ of the sequence $\left[\Omega_{g^\epsilon_{n(m)}}, y^\epsilon_{n(m)}\right]$ in the original cost (2.3) is again an obvious consequence of (3.5), by the positivity of the penalization term(s). $\square$

Corollary 3.1. *Assume that $L = 0$. Then the shape optimization problem (2.1) - (2.3) is equivalent with the optimal control problem in D, given by (3.1) - (3.3)* *and (2.10) - (2.12), completed by the state-control constraint*

$$\int_{I_g} \left[\nabla y(\mathbf{z}(t)) \cdot \frac{\nabla g(\mathbf{z}(t))}{|\nabla g(\mathbf{z}(t))|} - \alpha(\mathbf{z}(t)) \right]^2 |\mathbf{z}'(t)| dt = 0.$$

The equivalence is valid for general L, if we replace the second term in (3.1) by $\int_D [1 - H(g(\mathbf{x}))] L(\mathbf{x}, y(\mathbf{x}))\, d\mathbf{x}$.

Proof. Notice that, if the above constraint is fulfilled and $L = 0$, then the cost functional (3.1) is identical with (2.3) computed for Ω_g. We also use that the support of the control action in (3.2) is in $D \setminus \Omega_g$ and the constraint is equivalent with (2.2).

Any admissible triple $[y, g, u]$ for the control problem (3.1) - (3.3), and (2.10) - (2.12) together with the above constraint, generates an admissible pair $[\Omega_g, y_{\Omega_g}]$ for the shape optimization problem (2.1) - (2.3), with the same cost for $L = 0$. Conversely, from (3.4), we see that any admissible pair of the shape optimization problem can be extended to an admissible pair to the constrained control problem in D, with the same cost, for $L = 0$.

The second statement has a similar argument: the admissible elements for both problems are in one-to-one correspondence and the associated costs are the same since the functionals to be minimized are identical. $\square$

Remark 3.1. *In general, fixed domain methods provide just approximation techniques in shape optimization or free boundary problems, but here we get even equivalence, for general shape optimization problems and with respect to certain associated optimal control problems with constraints, defined in D. The penalization term in (3.1) represents exactly the application of standard mathematical programming techniques to the equality constraint introduced in Corollary 3.1.*

We continue now with the observation that, by the Weierstrass theorem, there is $m_g > 0$ (depending on g) such that (2.9) becomes

$$|\nabla g(\mathbf{x})| \geq m_g, \quad \forall \mathbf{x} \in G_g, \quad \forall g \in \mathcal{F}. \tag{3.6}$$

In order to strengthen the approximation property in Proposition 3.1, we impose that $\mathcal{F}$ is bounded in $\mathcal{C}^2(\overline{D})$ and we require uniformity in (2.9), (3.6), where

$m > 0$ is some given constant:

$$|\nabla g(\mathbf{x})| \geq m, \quad \forall \mathbf{x} \in G_g, \quad \forall g \in \mathcal{F}. \tag{3.7}$$

We denote by $y_{n,\epsilon}$ the solution of (2.1), (2.2) in the unknown domain $\Omega_{g_n^\epsilon}$ and we recall that $[y_n^\epsilon, g_n^\epsilon, u_n^\epsilon]$ are defined in Prop. 3.1 and are computed in D. The difference of the two states can be estimated in an advantageous way.

Proposition 3.2. *Under the assumption (3.7) and the boundedness of $\mathcal{F}$ in $\mathcal{C}^2(\overline{D})$, there is a constant $C > 0$, independent of $g_n^\epsilon \in \mathcal{F}$, such that*

$$|y_{n,\epsilon} - y_n^\epsilon|_{H^1(\Omega_{g_n^\epsilon})} \leq C\epsilon^{1/4}.$$

Proof. We take the difference of the equations (2.1) in $\Omega_{g_n^\epsilon}$ corresponding to $y_{n,\epsilon}$, y_n^ϵ and we multiply by $y_{n,\epsilon} - y_n^\epsilon$. Then, we get:

$$|y_{n,\epsilon} - y_n^\epsilon|^2_{H^1(\Omega_{g_n^\epsilon})} = -\int_{\partial\Omega_{g_n^\epsilon}} \left(\frac{\partial y_n^\epsilon}{\partial \mathbf{n}}\right)(y_{n,\epsilon} - y_n^\epsilon)d\sigma \leq c\epsilon^{1/2}|y_{n,\epsilon} - y_n^\epsilon|_{L^2(\partial\Omega_{g_n^\epsilon})},$$

where $c > 0$ is a constant, independent of $g_n^\epsilon \in \mathcal{F}$, and the boundedness of $\frac{\partial y_n^\epsilon}{\partial \mathbf{n}}$ in $L^2(\partial\Omega_{g_n^\epsilon})$ is given by the last statement in Proposition 3.1.

By (3.7) and Green's formula, we have:

$$\begin{aligned}
&m|y_{n,\epsilon} - y_n^\epsilon|^2_{L^2(\partial\Omega_{g_n^\epsilon})} \leq \int_{\partial\Omega_{g_n^\epsilon}} |y_{n,\epsilon} - y_n^\epsilon|^2 \, |\nabla g_n^\epsilon| d\sigma \\
&= \int_{\partial\Omega_{g_n^\epsilon}} |y_{n,\epsilon} - y_n^\epsilon|^2 \nabla g_n^\epsilon \cdot \nu_\epsilon d\sigma \\
&\leq \int_{\Omega_{g_n^\epsilon}} |y_{n,\epsilon} - y_n^\epsilon|^2 |\Delta g_n^\epsilon| dx + 2\int_{\Omega_{g_n^\epsilon}} |y_{n,\epsilon} - y_n^\epsilon||\nabla(y_{n,\epsilon} - y_n^\epsilon) \cdot \nabla g_n^\epsilon| dx \\
&\leq M[|y_{n,\epsilon} - y_n^\epsilon|^2_{L^2(\Omega_{g_n^\epsilon})} + |y_{n,\epsilon} - y_n^\epsilon|_{L^2(\Omega_{g_n^\epsilon})}|\nabla(y_{n,\epsilon} - y_n^\epsilon)|_{L^2(\Omega_{g_n^\epsilon})}] \\
&\leq M[|y_{n,\epsilon} - y_n^\epsilon|^2_{L^2(\Omega_{g_n^\epsilon})} + \epsilon^{1/2}|\nabla(y_{n,\epsilon} - y_n^\epsilon)|^2_{L^2(\Omega_{g_n^\epsilon})} \\
&+\epsilon^{-1/2}|y_{n,\epsilon} - y_n^\epsilon|^2_{L^2(\Omega_{g_n^\epsilon})}],
\end{aligned}$$

where we also use the binomial inequality (with the same ϵ as in Proposition 3.1) together with the boundedness of $\mathcal{F}$ in $\mathcal{C}^2(\overline{D})$. The notation ν_ϵ is the normal to $\partial\Omega_{g_n^\epsilon}$.

Combining the above two inequalities, we end the proof. $\square$

Remark 3.2. *We note the very weak hypotheses on the cost functional in Proposition 3.1. Together with Corollary 3.1 and Proposition 3.2, which gives an estimate independent of the geometry, the justification for the use of the control problem (3.1)-(3.3), (2.5) in the approximation of ($\mathcal{P}$), is obtained. A detailed study of the convergence properties when $\epsilon \to 0$, for a distributed cost functional, is performed in [47].*

Proposition 3.3. *Under the assumption (3.7) and the boundedness of $\mathcal{F}$ in $\mathcal{C}^1(\overline{D})$, the shape optimization problem has at least one optimal solution Ω^*.*

Proof. Condition (3.7) allows to apply the implicit function theorem around any point $\mathbf{x} = (x_1, x_2) \in G$ and to obtain the local representation of G via some function $x_2 = x_2(x_1)$. In particular, also taking into account the boundedness of $\mathcal{F}$ in $\mathcal{C}^1(\overline{D})$, it yields that $x_2'(x_1) = -\frac{g_{x_1}(x_1, x_2(x_1))}{g_{x_2}(x_1, x_2(x_1))}$ is bounded, uniformly with respect to the family of admissible domains, under appropriate choices of the local axes. This allows the application of well known existence results due to Chenais (see [39], Ch. 3.3) and to end the proof. $\square$

For general existence results in shape optimization, using just the uniform segment property, we quote [44], [33].

4. Directional derivative

We consider now functional variations $g + \lambda r$, $u + \lambda v$, $g, r \in \mathcal{F}$, $\lambda \in \mathbb{R}$, $u, v \in L^p(D)$. In the sequel, we shall take into account the condition (2.6), (2.7) for g, r in the identification of the corresponding domains from (2.4). This is also necessary in (2.10)-(2.12) and at the numerical level it is very easy to implement (finding some $\mathbf{x}_0$ arises to solve $g(\mathbf{x}) = 0$, which is a standard routine, and to use (2.10)-(2.12) to identify by elimination such initial conditions on each connected component of G_g; see [29] for such details). Notice that the perturbations of u are always admissible since we have no constraints on u and the perturbations of g satisfy (2.7) by definition and (2.9), (2.13) for $|\lambda|$ small enough (depending on g), due to the Weierstrass theorem applied in a closed neighborhood of G_g, respectively on ∂D.

We denote by $y_\lambda \in W^{2,p}(D)$, $\mathbf{z}_\lambda \in \mathcal{C}^1(\mathbb{R})^2$ the solutions of (3.2), (3.3) and (2.10)-(2.12) corresponding to the above variations, respectively. From the previous section, we know that $\mathbf{z}_\lambda$ is periodic with some period $T_\lambda > 0$ and we take its definition interval to be $[0, T_\lambda]$. In [29], Proposition 2.6, it is proved under conditions (2.9), (2.13), that $T_\lambda \to T_g$ as $\lambda \to 0$, where T_g is independent of r as the period of $\mathbf{z}$, i.e. $I_g = [0, T_g]$.

Proposition 4.1. *The system in variations corresponding to (3.2), (3.3), (2.10)-(2.12) is:*

$$
\begin{aligned}
-\Delta q + q &= g_+^2 v + 2g_+ u\, r, \quad \textit{in } D, &(4.1)\\
q &= 0, \quad \textit{on } \partial D, &(4.2)\\
w_1' &= -\nabla \partial_2 g(\mathbf{z}) \cdot \mathbf{w} - \partial_2 r(\mathbf{z}), \quad \textit{in } [0, T_g], &(4.3)\\
w_2' &= \nabla \partial_1 g(\mathbf{z}) \cdot \mathbf{w} + \partial_1 r(\mathbf{z}), \quad \textit{in } [0, T_g], &(4.4)\\
w_1(0) &= 0,\ w_2(0) = 0, &(4.5)
\end{aligned}
$$

where $q = \lim_{\lambda \to 0} \frac{y_\lambda - y}{\lambda}$, $\mathbf{w} = [w_1, w_2] = \lim_{\lambda \to 0} \frac{\mathbf{z}_\lambda - \mathbf{z}}{\lambda}$ *and the limits exist in* $W^{2,p}(D)$, *respectively* $\mathcal{C}^1([0, T_g])^2$.

Proof. We consider the perturbations of the parameters (controls) $g + \lambda r$, $u + \lambda v$ and the system (4.1)-(4.5) characterizes the variations of the corresponding solutions of the state system (3.2), (3.3), (2.10)-(2.12). For linear elliptic equations and for ordinary differential equations, this is known and we quote [29], [45], where relevant arguments can be found. $\square$

Proposition 4.2. *Under the assumption (2.9), we have:*

$$\lim_{\lambda \to 0} \frac{T_\lambda - T_g}{\lambda} = -\frac{w_2(T_g)}{z_2'(T_g)}$$

if $z_2'(T_g) \neq 0$.

Proof. Clearly $\nabla(g + \lambda r) \neq 0$ on $G_\lambda = \{\mathbf{x}; (g + \lambda r)(\mathbf{x}) = 0\}$ if $|\lambda|$ small, due to [47], Section 2, and the Weierstrass theorem. Notice that G_λ is non-empty for $|\lambda|$ small since g changes sign in D and $\lambda r \to 0$ uniformly in D

(and G_λ is close to G_g, in fact). By the variant of the Hamiltonian system (2.10)-(2.12) corresponding to $g + \lambda r$ it yields $|z_1^{\lambda\prime}(T_\lambda)| + |z_2^{\lambda\prime}(T_\lambda)| > 0$ and, similarly $|z_1'(T_g)| + |z_2'(T_g))| > 0$, due to (2.9). We choose here $z_2'(T_g) \neq 0$ and, consequently, $z_2^{\lambda\prime}(T_\lambda) \neq 0$, for λ "small". Then z_2^λ is invertible on some interval $[T_g - \sigma, T_g + \beta]$ with $\sigma, \beta > 0$, small, not depending on λ, (and similarly around 0 due to the periodicity property).

This is due to $\mathbf{z}_\lambda \to \mathbf{z}$ in $\mathcal{C}^1([0, 2T_g])^2$ and $T_\lambda \to T_g$. We have $\mathbf{z}_\lambda(T_\lambda) = \mathbf{x}_0$ and it yields:

$$T_\lambda = (z_2^\lambda)^{-1}(x_0^2). \tag{4.6}$$

We denote $x_0^\lambda = z_2(T_\lambda) \to x_0^2$ as $\lambda \to 0$. We may write for $\lambda \neq 0$

$$\frac{T_\lambda - T_g}{\lambda} = \frac{(z_2^\lambda)^{-1}(x_0^2) - (z_2)^{-1}(x_0^2)}{\lambda} = \frac{(z_2)^{-1}(x_0^\lambda) - (z_2)^{-1}(x_0^2)}{\lambda}. \tag{4.7}$$

By (4.6), (4.7) we get

$$\frac{T_\lambda - T_g}{\lambda} = \frac{(z_2)^{-1}(x_0^\lambda) - (z_2)^{-1}(x_0^2)}{x_0^\lambda - x_0^2} \frac{z_2(T_\lambda) - z_2^\lambda(T_\lambda)}{\lambda}.$$

Passing to the limit $\lambda \to 0$ in the above relation and using Proposition 4.1, we end the proof. $\square$

Remark 4.1. *If $z_1'(T_g) \neq 0$, the limit is $-\frac{w_1(T_g)}{z_1'(T_g)}$. In general, we denote by $\theta(g, r)$ this limit. The last condition in Proposition 4.2 or this condition here follow by (2.9).*

To study the differentiability properties of the penalized cost function (3.1), we also assume $f \in W^{1,p}(D)$, ∂D is in $\mathcal{C}^{2,1}$ and $\mathcal{F} \subset \mathcal{C}^2(\overline{D})$. By properties of the positive part, we get that $g_+^2 \in W^{1,\infty}(D)$ and $g_+^2 u \in W^{1,p}(D)$ if $u \in W^{1,p}(D)$ and the solution of (3.2), (3.3) satisfies, by the regularity properties of linear elliptic equations, that $y \in W^{3,p}(D) \subset \mathcal{C}^2(\overline{D})$ (due to the Sobolev theorem). The derivative that we obtain below, associated to functional variations, combines shape variations with topological variations.

Proposition 4.3. *Under the above conditions, assume that $J(\mathbf{x}, \cdot)$, $L(\mathbf{x}, \cdot)$ are in $\mathcal{C}^1(\mathbb{R})$, $j(\cdot, \cdot)$ is in $\mathcal{C}^1(\mathbb{R}^3)$ and α is in $\mathcal{C}^1(\mathbb{R}^2)$. Then, the directional derivative* *of the penalized cost functional (3.1), in the direction* $[v, r] \in W^{1,p}(D) \times \mathcal{F}$, *is given by:*

$$
\begin{aligned}
& \theta(g,r)\left[j(\mathbf{x}_0, y(\mathbf{x}_0)) + \frac{1}{\epsilon}\left| \frac{\partial y}{\partial \mathbf{n}}(\mathbf{x}_0) - \alpha(\mathbf{x}_0) \right|^2 \right] |\nabla g(\mathbf{x}_0)| \\
+ \quad & \int_E \partial_2 J(\mathbf{x}, y(\mathbf{x})) q(\mathbf{x}) d\mathbf{x} \\
+ \quad & \int_D [1 - H^\epsilon(g)] \partial_2 L(\mathbf{x}, y(\mathbf{x})) q(\mathbf{x}) d\mathbf{x} - \int_D L(\mathbf{x}, y(\mathbf{x}))(H^\epsilon)'(g(\mathbf{x})) r(\mathbf{x}) d\mathbf{x} \\
+ \quad & \int_0^{T_g} \nabla_1 j\left(\mathbf{z}(t), y(\mathbf{z}(t))\right) \cdot \mathbf{w}(t) |\mathbf{z}'(t)| dt \\
+ \quad & \int_0^{T_g} \partial_2 j\left(\mathbf{z}(t), y(\mathbf{z}(t))\right) \left[\nabla y(\mathbf{z}(t)) \cdot \mathbf{w}(t) + q(\mathbf{z}(t))\right] |\mathbf{z}'(t)| dt \\
+ \quad & \int_0^{T_g} j\left(\mathbf{z}(t), y(\mathbf{z}(t))\right) \frac{\mathbf{z}'(t) \cdot \mathbf{w}'(t)}{|\mathbf{z}'(t)|} dt \\
+ \quad & \frac{2}{\epsilon} \int_0^{T_g} \left(\nabla y(\mathbf{z}(t)) \cdot \frac{\nabla g(\mathbf{z}(t))}{|\nabla g(\mathbf{z}(t))|} - \alpha(\mathbf{z}(t)) \right) \frac{\nabla r(\mathbf{z}(t))}{|\nabla g(\mathbf{z}(t))|} \cdot \nabla y(\mathbf{z}(t)) |\mathbf{z}'(t)| dt \\
- \quad & \frac{2}{\epsilon} \int_0^{T_g} \left(\nabla y(\mathbf{z}(t)) \cdot \frac{\nabla g(\mathbf{z}(t))}{|\nabla g(\mathbf{z}(t))|} - \alpha(\mathbf{z}(t)) \right) \nabla \alpha(\mathbf{z}(t)) \cdot \mathbf{w}(t) |\mathbf{z}'(t)| dt \\
+ \quad & \frac{2}{\epsilon} \int_0^{T_g} \left(\nabla y(\mathbf{z}(t)) \cdot \frac{\nabla g(\mathbf{z}(t))}{|\nabla g(\mathbf{z}(t))|} - \alpha(\mathbf{z}(t)) \right) \left[\left(H\, y(\mathbf{z}(t))\right) \mathbf{w}(t) \right] \cdot \frac{\nabla g(\mathbf{z}(t))}{|\nabla g(\mathbf{z}(t))|} |\mathbf{z}'(t)| dt \\
+ \quad & \frac{2}{\epsilon} \int_0^{T_g} \left(\nabla y(\mathbf{z}(t)) \cdot \frac{\nabla g(\mathbf{z}(t))}{|\nabla g(\mathbf{z}(t))|} - \alpha(\mathbf{z}(t)) \right) \nabla q(\mathbf{z}(t)) \cdot \frac{\nabla g(\mathbf{z}(t))}{|\nabla g(\mathbf{z}(t))|} |\mathbf{z}'(t)| dt \\
+ \quad & \frac{2}{\epsilon} \int_0^{T_g} \left(\nabla y(\mathbf{z}(t)) \cdot \frac{\nabla g(\mathbf{z}(t))}{|\nabla g(\mathbf{z}(t))|} - \alpha(\mathbf{z}(t)) \right) \nabla y(\mathbf{z}(t)) \cdot \left[\frac{\left(H\, g(\mathbf{z}(t))\right) \mathbf{w}(t)}{|\nabla g(\mathbf{z}(t))|} \right. \\
& \left. - \frac{\nabla g(\mathbf{z}(t))}{|\nabla g(\mathbf{z}(t))|^3} \Big(\nabla g(\mathbf{z}(t)) \cdot \nabla r(\mathbf{z}(t)) + \nabla g(\mathbf{z}(t)) \cdot \left(H\, g(\mathbf{z}(t))\right) \mathbf{w}(t) \Big) \right] |\mathbf{z}'(t)| dt \\
+ \quad & \frac{1}{\epsilon} \int_0^{T_g} \left[\nabla y(\mathbf{z}(t)) \cdot \frac{\nabla g(\mathbf{z}(t))}{|\nabla g(\mathbf{z}(t))|} - \alpha(\mathbf{z}(t)) \right]^2 \frac{\mathbf{z}'(t) \cdot \mathbf{w}'(t)}{|\mathbf{z}'(t)|} dt. \qquad (4.8)
\end{aligned}
$$

Above $\nabla_1 j$ is the gradient of $j(\cdot, \cdot)$ with respect to the two components of $\mathbf{z}$, and $\partial_2 j$ is the partial derivative with respect to y, other quantities are defined in (4.1)-(4.5) and $H\, y$ is the Hessian matrix of $y \in \mathcal{C}^2(\overline{D})$, etc.

Proof. We compute

$$
\begin{aligned}
&\lim_{\lambda\to 0}\frac{1}{\lambda}\Big\{\int_E J(\mathbf{x},y_\lambda(\mathbf{x}))d\mathbf{x}+\int_D[1-H^\epsilon(g+\lambda r)(\mathbf{x})]L(\mathbf{x},y_\lambda(\mathbf{x}))d\mathbf{x}\\
&+\int_0^{T_\lambda} j\left(\mathbf{z}_\lambda(t),y_\lambda(\mathbf{z}_\lambda(t))\right)|\mathbf{z}_\lambda'(t)|dt\\
&+\frac{1}{\epsilon}\int_0^{T_\lambda}\left[\nabla y_\lambda(\mathbf{z}_\lambda(t))\cdot\frac{\nabla(g+\lambda r)(\mathbf{z}_\lambda(t))}{|\nabla(g+\lambda r)(\mathbf{z}_\lambda(t))|}-\alpha(\mathbf{z}_\lambda(t))\right]^2|\mathbf{z}_\lambda'(t)|dt\\
&-\int_E J(\mathbf{x},y(\mathbf{x}))d\mathbf{x}-\int_D[1-H^\epsilon(g)(\mathbf{x})]L(\mathbf{x},y(\mathbf{x}))d\mathbf{x}\\
&-\int_0^{T_g} j\left(\mathbf{z}(t),y(\mathbf{z}(t))\right)|\mathbf{z}'(t)|dt\\
&-\frac{1}{\epsilon}\int_0^{T_g}\left[\nabla y(\mathbf{z}(t))\cdot\frac{\nabla g(\mathbf{z}(t))}{|\nabla g(\mathbf{z}(t))|}-\alpha(\mathbf{z}(t))\right]^2|\mathbf{z}'(t)|dt\Big\}.
\end{aligned}
$$

Applying Proposition 4.1, (4.1), (4.2), and the differentiability hypotheses on J, L, we get:

$$\frac{1}{\lambda}\left[\int_E J(\mathbf{x},y_\lambda(\mathbf{x}))d\mathbf{x}-\int_E J(\mathbf{x},y(\mathbf{x}))d\mathbf{x}\right]\to\int_E\partial_2 J(\mathbf{x},y(\mathbf{x}))q(\mathbf{x})d\mathbf{x},\tag{4.9}$$

$$
\begin{aligned}
&\frac{1}{\lambda}\left[\int_D[1-H^\epsilon(g+\lambda r)]L(\mathbf{x},y_\lambda(\mathbf{x}))d\mathbf{x}-\int_D[1-H^\epsilon(g)]L(\mathbf{x},y(\mathbf{x}))d\mathbf{x}\right]\\
\to\quad&\int_D[1-H^\epsilon(g)]\partial_2 L(\mathbf{x},y(\mathbf{x}))q(\mathbf{x})d\mathbf{x}\\
&-\int_D L(\mathbf{x},y(\mathbf{x}))(H^\epsilon)'(g(\mathbf{x}))r(\mathbf{x})d\mathbf{x}.
\end{aligned}\tag{4.10}
$$

We discuss now the term:

$$
\begin{aligned}
&\frac{1}{\lambda}\int_{T_g}^{T_\lambda} j\left(\mathbf{z}_\lambda(t),y_\lambda(\mathbf{z}_\lambda(t))\right)|\mathbf{z}_\lambda'(t)|dt=\frac{T_\lambda-T_g}{\lambda}j\left(\mathbf{z}_\lambda(\tau_\lambda),y_\lambda(\mathbf{z}_\lambda(\tau_\lambda))\right)|\mathbf{z}_\lambda'(\tau_\lambda)|\\
&\to\theta(g,r)j(\mathbf{x}_0,y(\mathbf{x}_0))|\mathbf{z}'(T_g)|=\theta(g,r)j(\mathbf{x}_0,y(\mathbf{x}_0))|\nabla g(\mathbf{x}_0)|,
\end{aligned}\tag{4.11}
$$

due to (2.10)-(2.12) and Remark 4.1. Here τ_λ is some intermediary point in the interval $[T_g,T_\lambda]$, depending on λ, g, r, j, etc. We also use Thm. 2.1 and $T_\lambda\to T_g$.

Similarly, we consider the term:

$$
\begin{aligned}
& \frac{1}{\lambda}\int_{T_g}^{T_\lambda}\left[\nabla y_\lambda(\mathbf{z}_\lambda(t))\cdot\frac{\nabla(g+\lambda r)(\mathbf{z}_\lambda(t))}{|\nabla(g+\lambda r)(\mathbf{z}_\lambda(t))|}-\alpha(\mathbf{z}_\lambda(t))\right]^2|\mathbf{z}_\lambda'(t)|dt\\
\to\quad & \theta(g,r)\left[\nabla y(\mathbf{x}_0)\cdot\frac{\nabla g(\mathbf{x}_0)}{|\nabla g(\mathbf{x}_0)|}-\alpha(\mathbf{x}_0)\right]^2|\nabla g(\mathbf{x}_0)|\\
=\quad & \theta(g,r)\left|\frac{\partial y}{\partial \mathbf{n}}(\mathbf{x}_0)-\alpha(\mathbf{x}_0)\right|^2|\nabla g(\mathbf{x}_0)|. \qquad (4.12)
\end{aligned}
$$

In the last two limits, the regularity properties of y, $\mathbf{z}$, y_λ, $\mathbf{z}_\lambda$ also play a key role.

Next, we investigate the last term:

$$
\begin{aligned}
& \frac{1}{\lambda}\Bigg\{\int_0^{T_g} j\left(\mathbf{z}_\lambda(t),y_\lambda(\mathbf{z}_\lambda(t))\right)|\mathbf{z}_\lambda'(t)|dt\\
& +\frac{1}{\epsilon}\int_0^{T_g}\left[\nabla y_\lambda(\mathbf{z}_\lambda(t))\cdot\frac{\nabla(g+\lambda r)(\mathbf{z}_\lambda(t))}{|\nabla(g+\lambda r)(\mathbf{z}_\lambda(t))|}-\alpha(\mathbf{z}_\lambda(t))\right]^2|\mathbf{z}_\lambda'(t)|dt\\
& -\int_0^{T_g} j\left(\mathbf{z}(t),y(\mathbf{z}(t))\right)|\mathbf{z}'(t)|dt\\
& -\frac{1}{\epsilon}\int_0^{T_g}\left[\nabla y(\mathbf{z}(t))\cdot\frac{\nabla g(\mathbf{z}(t))}{|\nabla g(\mathbf{z}(t))|}-\alpha(\mathbf{z}(t))\right]^2|\mathbf{z}'(t)|dt\Bigg\}
\end{aligned}
$$

Clearly, the terms containing $j(\cdot,\cdot)$ give the limit:

$$
\begin{aligned}
& \int_0^{T_g}\left[\nabla_1 j\left(\mathbf{z}(t),y(\mathbf{z}(t))\right)\cdot\mathbf{w}(t)+\partial_2 j\left(\mathbf{z}(t),y(\mathbf{z}(t))\right)\nabla y(\mathbf{z}(t))\cdot\mathbf{w}(t)\right]|\mathbf{z}'(t)|dt\\
+\quad & \int_0^{T_g}\partial_2 j\left(\mathbf{z}(t),y(\mathbf{z}(t))\right)q(\mathbf{z}(t))|\mathbf{z}'(t)|dt\\
+\quad & \int_0^{T_g} j\left(\mathbf{z}(t),y(\mathbf{z}(t))\right)\frac{\mathbf{z}'(t)\cdot\mathbf{w}'(t)}{|\mathbf{z}'(t)|}dt \qquad (4.13)
\end{aligned}
$$

by passing to the limit under the integral over $[0,T_g]$ and using the differentiability assumptions on j and Prop. 4.1.

Let us consider now the two terms corresponding to the penalization of Neumann boundary condition. We add and subtract advantageous terms and we compute step by step:

$$
\begin{aligned}
& \frac{1}{\lambda}\int_0^{T_g}\left\{\left[\nabla y_\lambda(\mathbf{z}_\lambda(t))\cdot\frac{\nabla(g+\lambda r)(\mathbf{z}_\lambda(t))}{|\nabla(g+\lambda r)(\mathbf{z}_\lambda(t))|}-\alpha(\mathbf{z}_\lambda(t))\right]^2\right. \\
& \left.-\left[\nabla y(\mathbf{z}(t))\cdot\frac{\nabla g(\mathbf{z}(t))}{|\nabla g(\mathbf{z}(t))|}-\alpha(\mathbf{z}(t))\right]^2\right\}|\mathbf{z}_\lambda'(t)|dt \\
= & \frac{1}{\lambda}\int_0^{T_g} S\left[\nabla y_\lambda(\mathbf{z}_\lambda(t))\cdot\frac{\nabla(g+\lambda r)(\mathbf{z}_\lambda(t))}{|\nabla(g+\lambda r)(\mathbf{z}_\lambda(t))|}-\nabla y(\mathbf{z}(t))\cdot\frac{\nabla g(\mathbf{z}(t))}{|\nabla g(\mathbf{z}(t))|}\right. \\
& \left.-\alpha(\mathbf{z}_\lambda(t))+\alpha(\mathbf{z}(t))\right]|\mathbf{z}_\lambda'(t)|dt \\
= & \int_0^{T_g} S\frac{\nabla r(\mathbf{z}_\lambda(t))}{|\nabla(g+\lambda r)(\mathbf{z}_\lambda(t))|}\cdot\nabla y_\lambda(\mathbf{z}_\lambda(t))|\mathbf{z}_\lambda'(t)|dt \\
& +\int_0^{T_g} S\frac{\nabla y_\lambda(\mathbf{z}_\lambda(t))-\nabla y(\mathbf{z}(t))}{\lambda}\cdot\frac{\nabla g(\mathbf{z}(t))}{|\nabla g(\mathbf{z}(t))|}|\mathbf{z}_\lambda'(t)|dt \\
& +\frac{1}{\lambda}\int_0^{T_g} S\left[\nabla y_\lambda(\mathbf{z}_\lambda(t))\cdot\frac{\nabla g(\mathbf{z}_\lambda(t))}{|\nabla(g+\lambda r)(\mathbf{z}_\lambda(t))|}-\nabla y_\lambda(\mathbf{z}_\lambda(t))\cdot\frac{\nabla g(\mathbf{z}(t))}{|\nabla(g)(\mathbf{z}(t))|}\right]|\mathbf{z}_\lambda'(t)|dt \\
& -\frac{1}{\lambda}\int_0^{T_g} S\left[\alpha(\mathbf{z}_\lambda(t))-\alpha(\mathbf{z}(t))\right]|\mathbf{z}_\lambda'(t)|dt \\
= & I+II+III+IV \qquad (4.14)
\end{aligned}
$$

where S is the sum

$$
\nabla y_\lambda(\mathbf{z}_\lambda(t))\cdot\frac{\nabla(g+\lambda r)(\mathbf{z}_\lambda(t))}{|\nabla(g+\lambda r)(\mathbf{z}_\lambda(t))|}+\nabla y(\mathbf{z}(t))\cdot\frac{\nabla g(\mathbf{z}(t))}{|\nabla g(\mathbf{z}(t))|}-\alpha(\mathbf{z}_\lambda(t))-\alpha(\mathbf{z}(t)).
$$

We have:

$$
\begin{aligned}
& \lim_{\lambda\to 0} I = 2\int_0^{T_g}\left[\nabla y(\mathbf{z}(t))\cdot\frac{\nabla g(\mathbf{z}(t))}{|\nabla g(\mathbf{z}(t))|}-\alpha(\mathbf{z}(t))\right]\frac{\nabla r(\mathbf{z}(t))}{|\nabla g(\mathbf{z}(t))|}\cdot\nabla y(\mathbf{z}(t))|\mathbf{z}'(t)|dt \\
& \lim_{\lambda\to 0} II = \\
& 2\int_0^{T_g}\left[\nabla y(\mathbf{z}(t))\cdot\frac{\nabla g(\mathbf{z}(t))}{|\nabla g(\mathbf{z}(t))|}-\alpha(\mathbf{z}(t))\right]\left[H\,y(\mathbf{z}(t))+\nabla q(\mathbf{z}(t))\right]\cdot\frac{\nabla g(\mathbf{z}(t))}{|\nabla g(\mathbf{z}(t))|}|\mathbf{z}'(t)|dt.
\end{aligned}
$$

Concerning part III, we get:

$$
\begin{aligned}
&\lim_{\lambda\to 0} III \\
= \quad & 2\int_0^{T_g} \left[\nabla y(\mathbf{z}(t)) \cdot \frac{\nabla g(\mathbf{z}(t))}{|\nabla g(\mathbf{z}(t))|} - \alpha(\mathbf{z}(t))\right] |\mathbf{z}'(t)| \nabla y(\mathbf{z}(t)) \cdot \left[\frac{(H\, g(\mathbf{z}(t)))\, \mathbf{w}(t)}{|\nabla g(\mathbf{z}(t))|}\right. \\
& \left. - \frac{\nabla g(\mathbf{z}(t))}{|\nabla g(\mathbf{z}(t))|^2} \left(\frac{\nabla g(\mathbf{z}(t)) \cdot \nabla r(\mathbf{z}(t))}{|\nabla g(\mathbf{z}(t))|} + \frac{\nabla g(\mathbf{z}(t)) \cdot (H\, g(\mathbf{z}(t)))\, \mathbf{w}(t)}{|\nabla g(\mathbf{z}(t))|}\right)\right] dt \\
= \quad & 2\int_0^{T_g} \left[\nabla y(\mathbf{z}(t)) \cdot \frac{\nabla g(\mathbf{z}(t))}{|\nabla g(\mathbf{z}(t))|} - \alpha(\mathbf{z}(t))\right] \nabla y(\mathbf{z}(t)) \cdot \left[\frac{(H\, g(\mathbf{z}(t)))\, \mathbf{w}(t)}{|\nabla g(\mathbf{z}(t))|}\right. \\
& \left. - \frac{\nabla g(\mathbf{z}(t))}{|\nabla g(\mathbf{z}(t))|^3} \left(\nabla g(\mathbf{z}(t)) \cdot \nabla r(\mathbf{z}(t)) + \nabla g(\mathbf{z}(t))\, (H\, g(\mathbf{z}(t)))\, \mathbf{w}(t)\right)\right] |\mathbf{z}'(t)| dt.
\end{aligned}
$$

For the term

$$
\lim_{\lambda\to 0} IV = -2\int_0^{T_g} \left[\nabla y(\mathbf{z}(t)) \cdot \frac{\nabla g(\mathbf{z}(t))}{|\nabla g(\mathbf{z}(t))|} - \alpha(\mathbf{z}(t))\right] \nabla \alpha(\mathbf{z}(t)) \cdot \mathbf{w}(t) |\mathbf{z}'(t)| dt. \tag{4.15}
$$

Finally, we have

$$
\begin{aligned}
& \int_0^{T_g} \left[\nabla y(\mathbf{z}(t)) \cdot \frac{\nabla g(\mathbf{z}(t))}{|\nabla g(\mathbf{z}(t))|} - \alpha(\mathbf{z}(t))\right]^2 \frac{|\mathbf{z}'_\lambda(t)| - |\mathbf{z}'(t)|}{\lambda} dt \\
\to \quad & \int_0^{T_g} \left[\nabla y(\mathbf{z}(t)) \cdot \frac{\nabla g(\mathbf{z}(t))}{|\nabla g(\mathbf{z}(t))|} - \alpha(\mathbf{z}(t))\right]^2 \frac{\mathbf{z}'(t) \cdot \mathbf{w}'(t)}{|\mathbf{z}'(t)|} dt.
\end{aligned} \tag{4.16}
$$

Summing up relations (4.9)-(4.16), we finish the proof of (4.8). □

Remark 4.2. *If the domain Ω_g is not simply connected, then the terms in relation (4.8) are transformed in finite sums, except the ones associated to the domains E, D and the first term. The integrals over $[0, T_g]$ initially appear due to the parametrization of the unknown boundary via the Hamiltonian system. However, in relation (4.8), the terms containing $\mathbf{w}$, $\mathbf{w}'$ seem not possible to be expressed as integrals over the unknown boundary since their dependence on $\mathbf{z}$ is not pointwise.*

We notice that the terms containing q in (4.8) can be written as

$$
\begin{aligned}
& \int_E \partial_2 J\left(\mathbf{x}, y(\mathbf{x})\right) q(\mathbf{x}) d\mathbf{x} + \int_D [1 - H^\epsilon(g)] \partial_2 L(\mathbf{x}, y(\mathbf{x})) q(\mathbf{x}) d\mathbf{x} \\
+ & \int_{\partial\Omega_g} \partial_2 j\left(s, y(s)\right) q(s) ds + \frac{2}{\epsilon} \int_{\partial\Omega_g} \left(\frac{\partial y(s)}{\partial \mathbf{n}} - \alpha(s)\right) \frac{\partial q(s)}{\partial \mathbf{n}} ds
\end{aligned} \tag{4.17}
$$

Denote by $\gamma \in L^2(D)$ the right hand-side in (4.1). There is an isomorphism between the spaces $L^2(D)$ and $H^2(D) \cap H_0^1(D)$, given by $\gamma \to q$. Then, (4.17) gives a linear continuous functional depending on $\gamma \in L^2(D)$ and there is a unique $p \in L^2(D)$ such that the functional in (4.17) can be written as $\int_D p\gamma d\mathbf{x}$. Consequently, we get ($q$ is redenoted by φ):

$$\begin{aligned} & \int_E \partial_2 J\left(\mathbf{x}, y(\mathbf{x})\right)\varphi(\mathbf{x})d\mathbf{x} + \int_D [1 - H^\epsilon(g)]\partial_2 L(\mathbf{x}, y(\mathbf{x}))\varphi(\mathbf{x})d\mathbf{x} \\ & + \int_{\partial\Omega_g} \partial_2 j\left(s, y(s)\right)\varphi(s)ds + \frac{2}{\epsilon}\int_{\partial\Omega_g}\left(\frac{\partial y(s)}{\partial \mathbf{n}} - \alpha(s)\right)\frac{\partial \varphi(s)}{\partial \mathbf{n}}ds \\ = & \int_D p(\mathbf{x})\left(-\Delta\varphi(\mathbf{x}) + \varphi(\mathbf{x})\right)d\mathbf{x}, \quad \forall \varphi \in H^2(D) \cap H_0^1(D). \end{aligned} \tag{4.18}$$

From (4.18), it is clear that $p \in L^2(D)$ satisfies

$$-\Delta p + p = \chi_E\, \partial_2 J\left(\cdot, y(\cdot)\right) + [1 - H^\epsilon(g)]\partial_2 L(\cdot, y(\cdot)) + \xi, \tag{4.19}$$

in the sense of distributions in D. In (4.19), χ_E is the characteristic function of E in D and ξ is in the dual of $H^2(D) \cap H_0^1(D)$, the functional expressed by the sum of the boundary integrals in (4.18).

In fact, (4.18) gives the definition of $p \in L^2(D)$ as transposition solution (very weak solution) of (4.19) to which, formally, the null boundary condition is added. This is the adjoint system associated to (4.1), (4.2) and the terms in (4.8) containing q.

The remaining of (4.8) contains $\mathbf{w}$, $\mathbf{w}'$ and $\theta(g, r)$ (that includes one component of the vector $\mathbf{w}(T)$ by Proposition 4.2). Notice that $\mathbf{w}'$ can be replaced by the right hand-side in (4.3), (4.4), that depends on $\mathbf{w}$ too. The terms including r or ∇r are not taken into account now (two such expressions appear from the replacement of $\mathbf{w}'$ via (4.3), (4.4), as well).

We define now the adjoint system for the vector function $\mathbf{m}(t) = [m_1(t), m_2(t)]$, corresponding to (4.3)-(4.5) and the terms in (4.8) containing $\mathbf{w}(t)$:

$$
\begin{aligned}
-\mathbf{m}'(t) \;=\;& A^*(t)\mathbf{m}(t) + |\mathbf{z}'(t)|\nabla_1 j\left(\mathbf{z}(t), y(\mathbf{z}(t))\right) \\
&+|\mathbf{z}'(t)|\partial_2 j\left(\mathbf{z}(t), y(\mathbf{z}(t))\right)\nabla y(\mathbf{z}(t)) \\
&-\frac{2}{\epsilon}|\mathbf{z}'(t)|\left[\nabla y(\mathbf{z}(t))\cdot\frac{\nabla g(\mathbf{z}(t))}{|\nabla g(\mathbf{z}(t))|} - \alpha(\mathbf{z}(t))\right]\nabla\alpha(\mathbf{z}(t)) \\
&+\frac{2}{\epsilon}|\mathbf{z}'(t)|\left[\nabla y(\mathbf{z}(t))\cdot\frac{\nabla g(\mathbf{z}(t))}{|\nabla g(\mathbf{z}(t))|} - \alpha(\mathbf{z}(t))\right]H^*\left(y(\mathbf{z}(t))\right)\frac{\nabla g(\mathbf{z}(t))}{|\nabla g(\mathbf{z}(t))|} \\
&+\frac{2}{\epsilon}|\mathbf{z}'(t)|\left[\nabla y(\mathbf{z}(t))\cdot\frac{\nabla g(\mathbf{z}(t))}{|\nabla g(\mathbf{z}(t))|} - \alpha(\mathbf{z}(t))\right]H^*\left(g(\mathbf{z}(t))\right)\frac{\nabla y(\mathbf{z}(t))}{|\nabla g(\mathbf{z}(t))|} \\
&-\frac{2}{\epsilon}|\mathbf{z}'(t)|\left[\nabla y(\mathbf{z}(t))\cdot\frac{\nabla g(\mathbf{z}(t))}{|\nabla g(\mathbf{z}(t))|} - \alpha(\mathbf{z}(t))\right]\nabla y(\mathbf{z}(t))\cdot\nabla g(\mathbf{z}(t)) \\
&H^*\left(g(\mathbf{z}(t))\right)\frac{\nabla g(\mathbf{z}(t))}{|\nabla g(\mathbf{z}(t))|^3} + j\left(\mathbf{z}(t), y(\mathbf{z}(t))\right)A^*(t)\frac{\mathbf{z}'(t)}{|\mathbf{z}'(t)|} \\
&+\frac{1}{\epsilon}\left[\nabla y(\mathbf{z}(t))\cdot\frac{\nabla g(\mathbf{z}(t))}{|\nabla g(\mathbf{z}(t))|} - \alpha(\mathbf{z}(t))\right]^2 A^*(t)\frac{\mathbf{z}'(t)}{|\mathbf{z}'(t)|},
\end{aligned}
\tag{4.20}
$$

$$
\begin{aligned}
m_1(T_g) \;=\;& 0, \\
m_2(T_g) \;=\;& -\frac{1}{z_2'(T_g)}\Bigg[j\left(\mathbf{z}(T_g), y(\mathbf{z}(T_g))\right) \\
&+\frac{1}{\epsilon}\left(\nabla y(\mathbf{z}(T_g))\cdot\frac{\nabla g(\mathbf{z}(T_g))}{|\nabla g(\mathbf{z}(T_g))|} - \alpha(\mathbf{z}(T_g))\right)^2\Bigg]|\nabla g(\mathbf{z}(T_g))|,
\end{aligned}
\tag{4.21}
$$

where $H^*(\cdot)$, $A^*(t)$ denote adjoint matrices of the Hessian matrix $H(\cdot)$, respectively

$$
A(t) = \begin{bmatrix} -\nabla\partial_2 g(\mathbf{z}(t)) \\ \nabla\partial_1 g(\mathbf{z}(t)) \end{bmatrix}
$$

and we also use in (4.20) the periodicity of $\mathbf{z}(t)$ from (2.10)-(2.12).

The equations (4.18)-(4.21) constitute the adjoint system for the penalized optimal control problem (3.1)-(3.3). By taking into account (4.18)-(4.21) and (4.8) one can obtain the gradient of the cost functional (3.1), after including as well the terms involving r, ∇r, as explained above. To avoid a too lengthy exposition, this is performed just in the next section, at the discretized level, to be used in the numerical examples computed in Section 6.

5. Finite element descent directions

Let $\mathcal{T}_h$ be a triangulation of D, where h is the mesh size. Since in (4.8) we have to compute the Hessian matrices of g and y, we use the piecewise cubic finite element $\mathbb{P}_3$ in $\mathcal{T}_h$ for the approximation of g and y, by g_h and y_h. For the control term u_h or for α_h, one can employ lower order finite elements, like continuous piecewise linear $\mathbb{P}_1$ or piecewise constant $\mathbb{P}_0$. But, for simplicity of presentation (to avoid the introduction of more FEM spaces), we employ $\mathbb{P}_3$, for u_h or α_h, too. See [13], [42] for a discussion of finite element spaces.

We define

$$\mathbb{W}_h = \{\varphi_h \in \mathcal{C}(\overline{D});\ \varphi_{h|T} \in \mathbb{P}_3(T),\ \forall T \in \mathcal{T}_h\}$$

of dimension $n = card(\mathbb{W}_h)$ and

$$\mathbb{V}_h = \{\varphi_h \in \mathbb{W}_h;\ \varphi_h = 0 \text{ on } \partial D\},$$

of dimension $n_0 = card(\mathbb{V}_h)$ which are finite element approximations of Hilbert spaces $\mathbb{W} = H^1(D)$, $\mathbb{V} = H_0^1(D)$, respectively.

The parametrization function g is approximated by the finite element function $g_h \in \mathbb{W}_h$, $g_h(\mathbf{x}) = \sum_{i\in I} G_i\phi_i(\mathbf{x})$ where $G = (G_i)_{i\in I} \in \mathbb{R}^n$ is a real vector and ϕ_i is the basis in $\mathbb{W}_h$. Similarly, we denote by $u_h \in \mathbb{W}_h$, $y_h \in \mathbb{V}_h$ and the associated vectors $U = (U_i)_{i\in I} \in \mathbb{R}^n$ and $Y = (Y_j)_{j\in I_0} \in \mathbb{R}^{n_0}$, the discretization of the control, respectively the state. The Neumann boundary condition, $\alpha \in W^{1,p}(D)$ with $p > 2$ will be approximated by $\alpha_h \in \mathbb{W}_h$.

For $g_h = \sum_{i\in I} G_i\phi_i$, we can define $\partial_1^h g_h$ which is an approximation of $\partial_1 g = \frac{\partial g}{\partial x_1}$ in a similar way as in [29], where the discrete derivative at the node A_i of $\mathcal{T}_h$ is a weighted average of the derivatives in the triangles T_j such that A_i is a node of $\overline{T}_j$ and the weights are the triangles areas. We can define Π_h^1 a square matrix of order n such that $\partial_1^h g_h = \sum_{i\in I} \left(\Pi_h^1 G\right)_i \phi_i$ and similarly Π_h^2 a square matrix of order n for the derivative with respect of x_2, i.e. $\partial_2^h g_h = \sum_{i\in I} \left(\Pi_h^2 G\right)_i \phi_i$. Using FreeFem++ [24], the matrices Π_h^1, Π_h^2 can be computed with the command `interpolate(...,op=dop)` with $dop = 1$, respectively $dop = 2$, where dop is a numerical parameter for computing the derivative of the basis functions with respect to x_1, respectively x_2.

We denote the objective function (3.1) by

$$\begin{aligned}\mathcal{J}(g,u) &= \int_E J\left(\mathbf{x}, y(\mathbf{x})\right) d\mathbf{x} + \int_{I_g} j\left(\mathbf{z}(t), y(\mathbf{z}(t))\right) |\mathbf{z}'(t)| dt \\ &\quad + \frac{1}{\epsilon} \int_{I_g} \left[\nabla y(\mathbf{z}(t)) \cdot \frac{\nabla g(\mathbf{z}(t))}{|\nabla g(\mathbf{z}(t))|} - \alpha(\mathbf{z}(t))\right]^2 |\mathbf{z}'(t)| dt \\ &\quad + \int_D [1 - H^\epsilon(g(\mathbf{x}))] L\left(\mathbf{x}, y(\mathbf{x})\right) d\mathbf{x}. \end{aligned} \tag{5.1}$$

We denote the first and the fourth terms of (5.1) by

$$t_1 = \int_E J\left(\mathbf{x}, y(\mathbf{x})\right) d\mathbf{x}, \quad t_4 = \int_D [1 - H^\epsilon(g(\mathbf{x}))] L\left(\mathbf{x}, y(\mathbf{x})\right) d\mathbf{x}.$$

The second and the third terms of (5.1) represent integrals on $\partial\Omega_g$, written in a way that highlights the dependence on the controls $g,\ u$ via $y,\ z,\ I_g$, but not on the unknown geometry. More precisely

$$t_2 = \int_{\partial\Omega_g} j\left(s, y(s)\right) ds, \quad t_3 = \int_{\partial\Omega_g} \left[\nabla y(s) \cdot \frac{\nabla g(s)}{|\nabla g(s)|} - \alpha(s)\right]^2 ds$$

and the computed objective function is $\mathcal{J} = t_1 + t_2 + \frac{1}{\epsilon} t_3 + t_4$.

We can solve numerically (2.10)-(2.12) by forward Euler scheme with a step $\Delta t > 0$ and initial condition $Z_0 = \mathbf{x}_0$, to get $Z_k = (Z_k^1, Z_k^2)^T$ an approximation of $\mathbf{z}_g(t_k)$, with $t_k = k\Delta t$, $k = 0, 1, \ldots$. This method is explicit of order $\mathcal{O}(\Delta t)$ and a limitation of the time step size is necessary as an absolute stability condition, see [41], Section 11.3.3. For a scalar equation, $y'(t) = \lambda y(t)$, $y(0) = 1$ with $\lambda < 0$, the time step condition is $0 < \Delta t < \frac{2}{|\lambda|}$. In the examples, we have fixed $\Delta t = 0.0005$.

We stop the algorithm when Z_m is "near" Z_0. We set the discretization of the periodic curve $\mathbf{z}_g$ to be such that $T = m\Delta t$. We put $Z = (Z^1, Z^2)^T$, with $Z^1 = (Z_k^1)_{1\le k\le m} \in \mathbb{R}^m$ and $Z^2 = (Z_k^2)_{1\le k\le m} \in \mathbb{R}^m$.

The system (4.3)-(4.5) is linear and it can be solved numerically by backward Euler scheme

$$W_k = W_{k-1} + \Delta t\, A_k W_k + \Delta t\, c_k \tag{5.2}$$

$$W_0 = (0,0)^T \tag{5.3}$$

for $k = 1, \ldots, m$, where $W_k = (W_k^1, W_k^2)^T$,

$$A_k = \begin{pmatrix} -\partial_1^h \partial_2^h g_h(Z_k) & -\partial_2^h \partial_2^h g_h(Z_k) \\ \partial_1^h \partial_1^h g_h(Z_k) & \partial_2^h \partial_1^h g_h(Z_k) \end{pmatrix}, \quad c_k = \begin{pmatrix} -\partial_2^h r_h(Z_k) \\ \partial_1^h r_h(Z_k) \end{pmatrix}.$$

We may assume that $(I - \Delta t\, A_k)^{-1}$ exists, where I is the unity matrix. This method is implicit of order $\mathcal{O}(\Delta t)$ and it has good stability properties, see [41].

Using (4.3)-(4.4), we can eliminate $\mathbf{w}'(t)$ from the fifth and the last line of (4.8) and we obtain that the directional derivative of (3.1) is equal to $\Gamma_w + \Gamma_r + \Gamma_q$, where: Γ_w is the sum of all the terms containing $\mathbf{w}$ (8 terms) and the first term containing $\theta(g, r)$, Γ_r is the sum of all terms containing $\nabla r = (\partial_1 r, \partial_2 r)^T$ (2 terms), $(-\partial_2 r, \partial_1 r)^T$ (2 terms) and r (1 term), Γ_q is the sum of all terms containing q (4 terms). We can write:

$$\begin{aligned} \Gamma_w &= \theta(g,r) \left[j(\mathbf{x}_0, y(\mathbf{x}_0)) + \frac{1}{\epsilon} \left| \frac{\partial y}{\partial \mathbf{n}}(\mathbf{x}_0) - \alpha(\mathbf{x}_0) \right|^2 \right] |\nabla g(\mathbf{x}_0)| \\ &\quad + \int_0^{T_g} b_1(t) w_1(t) + b_2(t) w_2(t) dt, \qquad (5.4) \\ \Gamma_r &= \int_0^{T_g} \lambda_1(t) \partial_1 r(\mathbf{z}(t)) + \lambda_2(t) \partial_2 r(\mathbf{z}(t)) dt \\ &\quad - \int_D L(\mathbf{x}, y(\mathbf{x}))(H^\epsilon)'(g(\mathbf{x})) r(\mathbf{x}) d\mathbf{x}. \qquad (5.5) \end{aligned}$$

We introduce a discrete adjoint schema of (5.2)-(5.3)

$$-M_{k+1} = -M_k + \Delta t\, A_k^T M_k + \Delta t\, b_k \qquad (5.6)$$

for $k = m-1, m-2 \ldots, 0$, with M_m given in (5.9), where $M_k = (M_k^1, M_k^2)^T$ and b_k is an approximation of $(b_1(t_k), b_2(t_k))^T$. We set $M^1 = (M_k^1)_{1 \le k \le m} \in \mathbb{R}^m$ and $M^2 = (M_k^2)_{1 \le k \le m} \in \mathbb{R}^m$. We can see M_k as an approximation of $\mathbf{m}$ from (4.20).

Lemma 5.1. *We have the equality*

$$\Delta t \sum_{k=0}^{m-1} b_k \cdot W_k + M_m^T (I - \Delta t\, A_m) W_m = \Delta t \sum_{k=1}^{m} c_k \cdot M_k. \qquad (5.7)$$

Proof. We take the scalar product of (5.2) by M_k and adding for $k = 1, \dots, m$, we get

$$\sum_{k=1}^{m} W_k \cdot M_k = \sum_{k=1}^{m} W_{k-1} \cdot M_k + \Delta t \sum_{k=1}^{m} M_k^T A_k W_k + \Delta t \sum_{k=1}^{m} c_k \cdot M_k.$$

Similarly for (5.6), W_k and adding for $k = 0, \dots, m-1$ to obtain

$$-\sum_{k=0}^{m-1} M_{k+1} \cdot W_k = -\sum_{k=0}^{m-1} M_k \cdot W_k + \Delta t \sum_{k=0}^{m-1} W_k^T A_k^T M_k + \Delta t \sum_{k=0}^{m-1} b_k \cdot W_k.$$

Subtracting the last two equalities and using that

$$M_k^T A_k W_k = M_k \cdot (A_k W_k) = (A_k W_k) \cdot M_k = W_k \cdot (A_k^T M_k) = W_k^T A_k^T M_k$$

and

$$\sum_{k=1}^{m} W_{k-1} \cdot M_k = \sum_{k=0}^{m-1} M_{k+1} \cdot W_k,$$

we get

$$W_m \cdot M_m = M_0 \cdot W_0 + \Delta t M_m^T A_m W_m - \Delta t W_0^T A_0^T M_0 + \Delta t \sum_{k=1}^{m} c_k \cdot M_k - \Delta t \sum_{k=0}^{m-1} b_k \cdot W_k.$$

Taking into account the initial condition (5.3), we get (5.7). $\square$

From Proposition 4.2, Remark 4.1 and the notations of the proof of Proposition 4.3, we have

$$\theta(g,r) = -\frac{w_2(T_g)}{z_2'(T_g)}, \text{ if } z_2'(T_g) \neq 0, \text{ or } \theta(g,r) = -\frac{w_1(T_g)}{z_1'(T_g)}, \text{ if } z_1'(T_g) \neq 0.$$

We set the discrete version of (4.21)

$$\begin{aligned} \mu_m = & -\frac{\Delta t}{Z_m^2 - Z_{m-1}^2} |\nabla^h g_h(Z_m)| \\ & \times \left[j\left(Z_m, y_h(Z_m)\right) + \frac{1}{\epsilon} \left(\nabla^h y_h(Z_m) \cdot \frac{\nabla^h g_h(Z_m)}{|\nabla g_h(Z_m)|} - \alpha_h(Z_m) \right)^2 \right] \end{aligned} \quad (5.8)$$

and

$$M_m = (I - \Delta t\, A_m^T)^{-1} (0, \mu_m)^T. \quad (5.9)$$

Remark 5.1. *We obtain that*

$$M_m^T\,(I-\Delta t\,A_m)\,W_m = W_m\cdot\left(I-\Delta t\,A_m^T\right)M_m = W_m\cdot(0,\mu_m)^T = W_m^2\mu_m$$

which is an approximation of the term

$$\theta(g,r)\left[j(\mathbf{x}_0,y(\mathbf{x}_0))+\frac{1}{\epsilon}\left|\frac{\partial y}{\partial \mathbf{n}}(\mathbf{x}_0)-\alpha(\mathbf{x}_0)\right|^2\right]|\nabla g(\mathbf{x}_0)|.$$

We can use the left Riemann sum [51] in order to compute the numerical integration over the interval $[0,T_g]$ in (5.4)

$$\int_0^{T_g} b_1(t)w_1(t)+b_2(t)w_2(t)dt \approx \Delta t\sum_{k=0}^{m-1} b_k\cdot W_k.$$

Remark 5.2. *From Lemma 5.1 and Remark 5.1, we have the approximation*

$$\Gamma_w \approx \Delta t\sum_{k=1}^{m} c_k\cdot M_k. \tag{5.10}$$

We have the notations: $r_h(\mathbf{x}) = \sum_{i\in I} R_i\phi_i(\mathbf{x})$, with $R=(R_i)_{i\in I}\in\mathbb{R}^n$, $\partial_1^h r_h(\mathbf{x}) = \sum_{i\in I}\left(\Pi_h^1 R\right)_i\phi_i(\mathbf{x})$ and $\partial_2^h r_h(\mathbf{x}) = \sum_{i\in I}\left(\Pi_h^2 R\right)_i\phi_i(\mathbf{x})$. By construction, we have $c_k = \left(-\partial_2^h r_h(Z_k), \partial_1^h r_h(Z_k)\right)^T$. Let us introduce the $n\times m$ matrix

$$\Phi(Z) = \left(\phi_i(Z_k)\right)_{i\in I, 1\le k\le m}.$$

We continue the computations in (5.7):

$$\begin{aligned}
\Delta t\sum_{k=1}^{m} c_k\cdot M_k &= \Delta t\sum_{k=1}^{m} -M_k^1\partial_2^h r_h(Z_k) + \Delta t\sum_{k=1}^{m} M_k^2\partial_1^h r_h(Z_k)\\
&= \Delta t\sum_{k=1}^{m} -M_k^1\sum_{i\in I}\left(\Pi_h^2 R\right)_i\phi_i(Z_k) + \Delta t\sum_{k=1}^{m} M_k^2\sum_{i\in I}\left(\Pi_h^1 R\right)_i\phi_i(Z_k)\\
&= -\Delta t\sum_{i\in I}\left(\Pi_h^2 R\right)_i\sum_{k=1}^{m}\phi_i(Z_k)M_k^1 + \Delta t\sum_{i\in I}\left(\Pi_h^1 R\right)_i\sum_{k=1}^{m}\phi_i(Z_k)M_k^2\\
&= -\Delta t\sum_{i\in I}\left(\Pi_h^2 R\right)_i\left(\Phi(Z)M^1\right)_i + \Delta t\sum_{i\in I}\left(\Pi_h^1 R\right)_i\left(\Phi(Z)M^2\right)_i\\
&= -\Delta t\left\langle \Pi_h^2 R, \Phi(Z)M^1\right\rangle_{\mathbb{R}^n} + \Delta t\left\langle \Pi_h^1 R, \Phi(Z)M^2\right\rangle_{\mathbb{R}^n}\\
&= -\Delta t\left\langle R, (\Pi_h^2)^T\Phi(Z)M^1\right\rangle_{\mathbb{R}^n} + \Delta t\left\langle R, (\Pi_h^1)^T\Phi(Z)M^2\right\rangle_{\mathbb{R}^n}\\
&= \left\langle R, -\Delta t(\Pi_h^2)^T\Phi(Z)M^1 + \Delta t(\Pi_h^1)^T\Phi(Z)M^2\right\rangle_{\mathbb{R}^n}. \qquad (5.11)
\end{aligned}$$

We follow a similar way for the approximation of the first term of Γ_r given by (5.5). We denote $\Lambda^1 = (\lambda_1(t_k))_{1\leq k\leq m}$ and $\Lambda^2 = (\lambda_2(t_k))_{1\leq k\leq m}$. We have

$$\begin{aligned} & \Delta t \sum_{k=1}^{m} \lambda_1(t_k)\partial_1^h r_h(Z_k) + \Delta t \sum_{k=1}^{m} \lambda_2(t_k)\partial_2^h r_h(Z_k) \\ = \quad & \left\langle R, \Delta t(\Pi_h^1)^T \Phi(Z)\Lambda^1 + \Delta t(\Pi_h^2)^T \Phi(Z)\Lambda^2 \right\rangle_{\mathbb{R}^n}. \end{aligned} \tag{5.12}$$

Setting

$$\Upsilon = \left(- \int_D L(\mathbf{x}, y(\mathbf{x}))(H^\epsilon)'(g(\mathbf{x}))\phi_i(\mathbf{x})d\mathbf{x} \right)_{i\in I}$$

the second term of Γ_r is approached by

$$\Upsilon \cdot R. \tag{5.13}$$

Let us introduce the discrete weak formulation of (4.1)-(4.2): find $q_h \in \mathbb{V}_h$ such that

$$\int_D \nabla q_h \cdot \nabla \varphi_h \, d\mathbf{x} + \int_D q_h \varphi_h \, d\mathbf{x} = \int_D (g_h)_+^2 v_h \varphi_h + 2(g_h)_+ u_h r_h \varphi_h \, d\mathbf{x}, \qquad \forall \varphi_h \in \mathbb{V}_h \tag{5.14}$$

and the corresponding discrete weak formulation of (4.18): find $p_h \in \mathbb{V}_h$ such that

$$\begin{aligned} & \int_D \nabla\varphi_h \cdot \nabla p_h d\mathbf{x} + \int_D \varphi_h p_h d\mathbf{x} = \int_E \partial_2 J\left(\mathbf{x}, y_h(\mathbf{x})\right)\varphi_h(\mathbf{x})d\mathbf{x} \\ & + \int_{\partial\Omega_{g_h}} \partial_2 j\left(s, y_h(s)\right)\varphi_h(s)ds + \int_D [1 - H^\epsilon(g_h)]\partial_2 L(\mathbf{x}, y_h(\mathbf{x}))\varphi_h(\mathbf{x})d\mathbf{x} \\ & + \frac{2}{\epsilon}\int_{\partial\Omega_{g_h}} \left(\nabla y_h(s) \cdot \frac{\nabla g_h(s)}{|\nabla g_h(s)|} - \alpha_h(s) \right) \nabla\varphi_h(s) \cdot \frac{\nabla g_h(s)}{|\nabla g_h(s)|} ds \end{aligned} \tag{5.15}$$

for all $\varphi_h \in \mathbb{V}_h$. In the right hand-side of (5.15), just the terms multiplying q in the gradient (4.8) appear. The H^1 error for the solution of elliptic problem like (5.14), when using $\mathbb{P}_3$ triangular finite element, has the order $\mathcal{O}(h^3)$, see [42].

Putting $\varphi_h = q_h$ in (5.15) and $\varphi_h = p_h$ in (5.14) we get

$$\begin{aligned}
& \int_E \partial_2 J\left(\mathbf{x}, y_h(\mathbf{x})\right) q_h(\mathbf{x}) d\mathbf{x} + \int_{\partial\Omega_{g_h}} \partial_2 j\left(s, y_h(s)\right) q_h(s) ds \\
& + \int_D [1 - H^\epsilon(g_h)] \partial_2 L(\mathbf{x}, y_h(\mathbf{x})) q_h(\mathbf{x}) d\mathbf{x} \\
& + \frac{2}{\epsilon} \int_{\partial\Omega_{g_h}} \left(\nabla y_h(s) \cdot \frac{\nabla g_h(s)}{|\nabla g_h(s)|} - \alpha_h(s) \right) \nabla q_h(s) \cdot \frac{\nabla g_h(s)}{|\nabla g_h(s)|} ds \\
= \; & \int_D \nabla q_h \cdot \nabla p_h \, d\mathbf{x} + \int_D q_h p_h \, d\mathbf{x} = \int_D (g_h)_+^2 v_h p_h + 2(g_h)_+ u_h r_h p_h \, d\mathbf{x} \\
= \; & P^T B V + P^T C R \qquad (5.16)
\end{aligned}$$

where B and C are two $n_0 \times n$ matrices defined by

$$B = \left(\int_D (g_h)_+^2 \phi_j \phi_i d\mathbf{x} \right)_{i \in I_0, j \in I}, \quad C = \left(\int_D 2(g_h)_+ u_h \phi_j \phi_i \, d\mathbf{x} \right)_{i \in I_0, j \in I}.$$

Using (5.11), (5.12), (5.13), (5.16), we obtain the result below.

Proposition 5.1. *The discrete version of (4.8) is:*

$$\begin{aligned}
d\mathcal{J}_{(G,U)}(R, V) \;=\; & \left\langle R, -\Delta t (\Pi_h^2)^T \Phi(Z) M^1 + \Delta t (\Pi_h^1)^T \Phi(Z) M^2 \right\rangle_{\mathbb{R}^n} \\
+ \; & \left\langle R, \Delta t (\Pi_h^1)^T \Phi(Z) \Lambda^1 + \Delta t (\Pi_h^2)^T \Phi(Z) \Lambda^2 \right\rangle_{\mathbb{R}^n} + \langle R, \Upsilon \rangle_{\mathbb{R}^n} \\
+ \; & \left\langle B^T P, V \right\rangle_{\mathbb{R}^n} + \left\langle C^T P, R \right\rangle_{\mathbb{R}^n}. \qquad (5.17)
\end{aligned}$$

Remark 5.3. *Due to (4.8) and Remark 4.2, if Ω_g is not simply connected, we have to take into account in (5.17) the sum of the terms corresponding to each component of $\partial\Omega_g$, computed as above. For a given g_h, the software FreeFem++ permits us, by using the command `isoline`, to get the number of connected components of the level set $g_h = 0$ and to get a point $\mathbf{x}_0$ on each connected component. The point $\mathbf{x}_0$ is used as initial condition in order to solve (2.10)-(2.12) by forward Euler scheme. If the domain Ω_g has small holes, the time step size and a numerical parameter for stoping the algorithm when we compute the period T_g have to be adapted by trial. Sometimes, in the case of very small holes, the algorithm fails at this stage of detecting the period and such very small holes are not taken into account.*

We use the general descent direction method

$$(G^{k+1}, U^{k+1}) = (G^k, U^k) + \lambda_k (R^k, V^k),$$

where $\lambda_k > 0$ is obtained via some line search

$$\lambda_k \in \arg\min_{\lambda > 0} \mathcal{J}\left((G^k, U^k) + \lambda(R^k, V^k)\right)$$

and (R^k, V^k) is a descent direction, i.e. $d\mathcal{J}_{(G^k,U^k)}(R^k, V^k) < 0$. For $E \neq \emptyset$, a projection of G^{k+1} is necessary in order to get (2.4). The algorithm stops if $|\mathcal{J}(G^{k+1}, U^{k+1}) - \mathcal{J}(G^k, U^k)| < tol$. Instead of the absolute difference between subsequent values of the cost function, we can use as well the relative error.

Other choices are possible, see [14] for details on such algorithms.

Corollary 5.1. *The opposite of the discrete gradient*

$$\begin{aligned} R^* &= \Delta t(\Pi_h^2)^T \Phi(Z) M^1 - \Delta t(\Pi_h^1)^T \Phi(Z) M^2 \\ &\quad -\Delta t(\Pi_h^1)^T \Phi(Z) \Lambda^1 - \Delta t(\Pi_h^2)^T \Phi(Z) \Lambda^2 - \Upsilon \\ &\quad -C^T P \\ V^* &= -B^T P \end{aligned}$$

yields the steepest descent direction (R^*, V^*) for $\mathcal{J}$ at (G, U).

Since the approximating state system (3.2), (3.3) is similar to [29], we also indicate here a similar simplified technique to get a partial descent direction, based only on a part of the discrete gradient in Corollary 5.1, (just the terms containing q in (4.8)).

Proposition 5.2. *Given $g_h, u_h \in \mathbb{W}_h$ and the variations $r_h, v_h \in \mathbb{W}_h$, let $y_h \in \mathbb{V}_h$ be the finite element solution of (3.2), (3.3), let $q_h \in \mathbb{V}_h$ be the finite element solution of (4.1), (4.2) depending on r_h, v_h and let $p_h \in \mathbb{V}_h$ be the solution of (5.15). Then*

$$\begin{aligned} &\int_E \partial_2 J(\mathbf{x}, y_h(\mathbf{x}))\, q_h(\mathbf{x}) d\mathbf{x} + \int_{\partial\Omega_{g_h}} \partial_2 j(s, y_h(s))\, q_h(s) ds \\ + &\int_D [1 - H^\epsilon(g_h)] \partial_2 L(\mathbf{x}, y_h(\mathbf{x})) q_h(\mathbf{x}) d\mathbf{x} \\ + &\frac{2}{\epsilon} \int_{\partial\Omega_{g_h}} \left(\nabla y_h(s) \cdot \frac{\nabla g_h(s)}{|\nabla g_h(s)|} - \alpha_h(s)\right) \nabla q_h(s) \cdot \frac{\nabla g_h(s)}{|\nabla g_h(s)|} ds \leq 0 \end{aligned} \quad (5.18)$$

if we choose:

i) $r_h = -p_h u_h$ *and* $v_h = -p_h$ *or*

ii) $r_h = -\widetilde{d}_h$ *and* $v_h = -p_h$ *where* $\widetilde{d}_h \in \mathbb{W}_h$ *is the solution of*

$$\int_D \nabla \widetilde{d}_h \cdot \nabla \varphi_h d\mathbf{x} + \int_D \widetilde{d}_h \varphi_h d\mathbf{x} \quad = \quad \int_D 2(g_h)_+ u_h p_h \varphi_h d\mathbf{x}, \forall \varphi_h \in \mathbb{W}_h \tag{5.19}$$

or

iii) $r_h = -\widehat{d}_h$ *and* $v_h = -p_h$ *where* $\widehat{d}_h \in \mathbb{V}_h$ *is the solution of*

$$\int_D \nabla \widehat{d}_h \cdot \nabla \varphi_h d\mathbf{x} \quad = \quad \int_D 2(g_h)_+ u_h p_h \varphi_h d\mathbf{x}, \ \forall \varphi_h \in \mathbb{V}_h. \tag{5.20}$$

Proof. In (5.16), we obtained that the left hand side of (5.18) is equal to:

$$\int_D (g_h)_+^2 v_h p_h d\mathbf{x} + \int_D 2(g_h)_+ u_h r_h p_h d\mathbf{x}.$$

For $v_h = -p_h$, we have

$$\int_D (g_h)_+^2 v_h p_h d\mathbf{x} = -\int_D (g_h)_+^2 p_h^2 d\mathbf{x} \leq 0.$$

If $(g_h)_+ p_h$ is not null, then the above inequality is strict.

Case i). For $r_h = -p_h u_h$, we have

$$\int_D 2(g_h)_+ u_h r_h p_h d\mathbf{x} = -\int_D 2(g_h)_+ (u_h p_h)^2 d\mathbf{x} \leq 0.$$

Case ii). For $r_h = -\widetilde{d}_h$, we have

$$\begin{aligned} \int_D 2(g_h)_+ u_h r_h p_h d\mathbf{x} &= -\int_D 2(g_h)_+ u_h p_h \widetilde{d}_h d\mathbf{x} \\ &= -\int_D \nabla \widetilde{d}_h \cdot \nabla \widetilde{d}_h d\mathbf{x} - \int_D \widetilde{d}_h \widetilde{d}_h d\mathbf{x} \leq 0. \end{aligned}$$

The second equality is obtained by putting $\varphi_h = \widetilde{d}_h$ in (5.19).

Case iii). For $r_h = -\widehat{d}_h$, we have

$$\begin{aligned} \int_D 2(g_h)_+ u_h r_h p_h d\mathbf{x} &= -\int_D 2(g_h)_+ u_h p_h \widehat{d}_h d\mathbf{x} \\ &= -\int_D \nabla \widehat{d}_h \cdot \nabla \widehat{d}_h d\mathbf{x} \leq 0. \end{aligned}$$

The second equality is obtained by putting $\varphi_h = \widehat{d}_h$ in (5.20). If $(g_h)_+ p_h$ is not null, then the inequality (5.18) is strict. This ends the proof. $\square$

The cases *ii)* and *iii)* are inspired by [12].

Remark 5.4. *The above methodology offers a systematic and general approximation procedure that can be applied in many examples and produces relevant results. Both topological and boundary variations are performed simultaneously. At the intuitive level, one may think just of the graph of a function $\hat{J}$ defined on a bidimensional domain D with one global maximum and several local maximums. Starting from the global maximum and having a descent direction, the level sets of $\hat{J}$ will evolve first from one point to a closed curve, then, when reaching the level of a lower local maximum, another closed curve, (disjoint from the previous one) will be added to the level line or, when reaching the common bottom of two neighboring peaks, two components of the level line will merge into one, etc. A similar evolution may happen with the null level line of $g + \lambda r$ when the parameter λ varies and we use the steepest descent direction $[r,\ v]$ for the cost functional $\mathcal{J}$, as in Corollary 5.1.*

6. Numerical tests

Optimal design problems are non convex and, in general, one may obtain numerically just a "local" solution of the penalized problem. The sense of "local" may be related to the Hausdorff-Pompeiu complementary topology of admissible domains, [33], or to the topology in the space of admissible controls g, u, etc. The computed penalization terms may remain not null, that is, the constraint (2.2) may be violated, but we also examine the numerical behavior of the original optimal design problem. An important and useful characteristic of the approximation methods from this paper is the descent property.

In the sequel, we discuss some academic examples related to the various problems and algorithmic approaches investigated in the previous sections. We employ the software FreeFem++, [24].

For the descent direction, we use Corollary 5.1 in Examples 1 and 3 and Proposition 5.2 in Example 2. The integrals on $\partial\Omega_g$ can be computed with the FreeFem++ command `int1d(Th,levelset=gh)(...)`, even if there are multiple connected components. For solving (2.10)-(2.12) by forward Euler scheme, we have used a small time step $\Delta t = 0.0005$. The formulas in Corollary 5.1 depend on m_j, the number of time steps in order to get the period $T_j = m_j \Delta t$ (generally, m_j is different for each connected component Γ_g^j of the boundary $\partial\Omega_g = \cup_{1\le j\le k_g}\Gamma_g^j$). Inspired by Proposition 3.2, in each example we calculate in a separate table the values of the cost in the original formulation of the problem, confirming the efficiency of this approach. This Section also shows that our approach can be applied under fairly general conditions (see Example 3a).

Example 1.

Case a). We set $D =]-3,3[\times]-3,3[$, $f = -1$, $\epsilon = 0.1$ and $y_d : D \to \mathbb{R}$ given by:

$$y_d(\mathbf{x}) = 0, \text{ if } \min\left(1 - x_1^2 - x_2^2, (x_1 - 1/2)^2 + x_2^2 - 1/64\right) > 0$$

and $y_d(\mathbf{x}) = -\frac{1}{\epsilon^2}$ otherwise. We fix $\alpha = 0$, a homogeneous Neumann boundary condition. We also set $J = 0$, $j = 0$ and $L(\mathbf{x}, y(\mathbf{x})) = \frac{1}{2}\left(y(\mathbf{x}) - y_d(\mathbf{x})\right)^2$. We use H^ϵ, a regularization of the Heaviside function, from [32]

$$H^\epsilon(r) = \begin{cases} 1, & r \ge 0, \\ \frac{\epsilon(r+\epsilon)^2 - 2r(r+\epsilon)^2}{\epsilon^3}, & -\epsilon < r < 0, \\ 0, & r \le -\epsilon \end{cases}$$

which satisfies the condition $H^\epsilon(r) = 1$, for $r > 0$, used in the proof of Proposition 3.1.

The objective function is $\mathcal{J} = \frac{1}{\epsilon} t_3 + t_4$ and the descent direction is given by the Corollary 5.1. The mesh of D has 78580 triangles and 39651 vertices and the tolerance parameter for the stopping test is $tol = 10^{-6}$.

We solve the line-search by

$$\min_{\lambda = \beta^i} \mathcal{J}\left((G^k, U^k) + \lambda(R^k, V^k)\right)$$

with $\beta = 0.8$ and $i = 0, \ldots, 29$. Consequently, at each iteration k, for the line-search, we evaluate the cost function 30 times. Later, for the Example 3, b), we use Armijo rule [10], at the line-search and the number of the cost function evaluations will be reduced.

Let (r_h^*, v_h^*) be the finite element direction associated to the descent direction (R^*, V^*) given by the Corollary 5.1. In order to augment the regularity of the r_h^*, we replace it by the solution of the elliptic problem: find $\widetilde{r}_h \in \mathbb{W}_h$ such that

$$\int_D \nabla \widetilde{r}_h \cdot \nabla \varphi_h d\mathbf{x} + \int_D \widetilde{r}_h \varphi_h d\mathbf{x} = \int_D r_h^* \varphi_h d\mathbf{x}, \quad \forall \varphi_h \in \mathbb{W}_h.$$

This technique is inspired by [12].

Different initial domains have been tested empirically in order to find initial domains for examples with changes of the topology or other properties of interest. For the initial domain given by $g_0(x_1, x_2) = x_1^2 + x_2^2 - 2^2$ and the initial control $u_0 = -1$, the algorithm succeeds to find the global solution here (the void set, due to the positivity of the cost, see Fig. 1) and stops at $k = 4$ iterations, because $\Omega_{g_5} = \emptyset$. We show in Table 1 the objective function, in Table 2 the values of t_4 for the finite element solution of the original state system (2.1), (2.2). Taking into account that the cost function is positive for non-empty domains, we stop the algorithm either by $|\mathcal{J}(G^{k+1}, U^{k+1}) - \mathcal{J}(G^k, U^k)| < tol$ or by $\Omega_{g_{k+1}} = \emptyset$.

Remark 6.1. *We also analyze the stopping criterion*

$$\frac{|\mathcal{J}(G^{k+1}, U^{k+1}) - \mathcal{J}(G^k, U^k)|}{|\mathcal{J}(G^k, U^k)|},$$

in Table 11, however the gradient type criterion $\|(R^k, V^k)\| < tol$ may give misleading information since the action of the gradient in the state system (3.2), for the computation of $\mathcal{J}\left((G^k, U^k) + \lambda(R^k, V^k)\right)$ during the line search, is limited to the fictitious part of the domain D and the other components of the vector (R^k, V^k) have no contribution to the minimization process and may be not relevant. In fact, (3.2) shows that the control action is given by products of the two controls and the admissible choices from (3.4) are not unique and not bounded. In this example and in Example 3, we employ around twenty gradient vectors $(R^k, V^k) \in \mathbb{R}^n \times \mathbb{R}^n$ and n is here $dim(W_h) = 354691$.

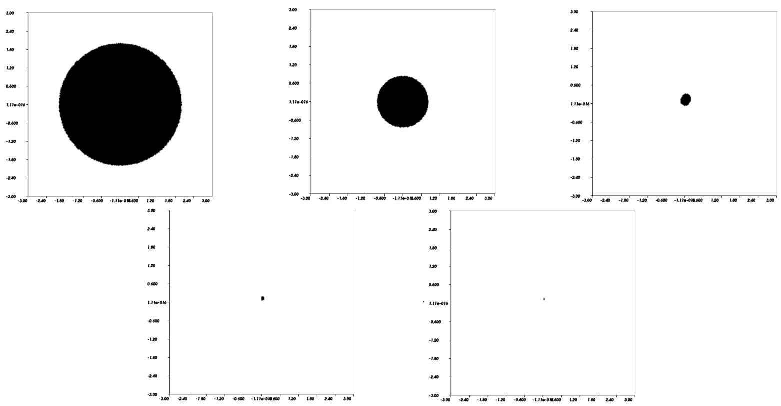

Figure 1: Example 1, case a). Initial domain $k = 0$ (top, left), domains for $k = 1$ (top, middle), $k = 2$ (top, right), $k = 3$ (bottom, left) and the domain (non optimal) for $k = 4$ (bottom, right). For $k = 5$, we obtain $\Omega_g = \emptyset$, not plotted here.

it.	k=0	k=1	k=2	k=3	k=4
t_3	31.1067	52.6968	1.44878	0.0762913	0.00676896
t_4	45107.2	286.1	14.1224	8.77257	8.30978
$\mathcal{J}$	45418.2	813.068	28.6102	9.53548	8.37747

Table 1: Example 1, case a). The computed objective function $\mathcal{J} = \frac{1}{\epsilon} t_3 + t_4$.

We notice that, for any admissible domain Ω_g, the solution of (2.1), (2.2) is $y(x) = -1$ as one can easily check. For $J = 0$, $j = 0$ and taking into account the form of L and y_d, we infer that the original cost (2.3) is strictly positive for any non-empty admissible domain. That is, this example has a unique global solution corresponding to $\Omega_g = \emptyset$, which is a rare situation in shape optimization. The algorithm succeeds to find a global solution in this example.

Case b). We set $D =]-5, 5[\times]-5, 5[$, $\alpha = 0$ and $y_d : D \to \mathbb{R}$ given by:

$$y_d(\mathbf{x}) = (x_1^2 + x_2^2 - 4)^2 (x_1^2 + x_2^2 - 1)^2, \text{ if } 1 < x_1^2 + x_2^2 < 4$$

it.	k=0	k=1	k=2	k=3	k=4
t_4	46292.1	241.582	0.0495296	0.004760	0.000230

Table 2: Example 1, case a). The values of t_4 for the finite element solution of the original state system (2.1), (2.2), in the domains presented in Figure 1.

and $y_d(\mathbf{x}) = 0$ otherwise. We also put

$$f(\mathbf{x}) = (x_1^2+x_2^2)^4 - 74(x_1^2+x_2^2)^3 + 393(x_1^2+x_2^2)^2 - 568(x_1^2+x_2^2) + 176, \text{ if } x_1^2+x_2^2 \leq 4$$

and $f(\mathbf{x}) = 0$ if $x_1^2 + x_2^2 > 4$. The other data is as above. Then, the global minimum value is again null and the void set is a global solution, as in the case a). However, it is easy to check that for any admissible domain including $\{(x_1, x_2) \in \mathbb{R}^2;\ 1 < x_1^2 + x_2^2 < 4\}$ and having the hole $\{(x_1, x_2) \in \mathbb{R}^2;\ 1 > x_1^2 + x_2^2\}$, y_d is the unique solution of (2.1), (2.2), that is the corresponding value of the cost (2.3) is again null. We see that this example admits an infinity of domains as global solutions, showing the difficulties at the computational level.

Example 2.

This example is based on the use of the Proposition 5.2 that offers some simplified choices for the descent directions. It has the advantage of simplicity, however such choices are not always possible and this gives here the stopping criterion of the algorithm.

Case a). We choose $D =]-3, 3[\times]-3, 3[$, $y_d(x_1, x_2) = x_1^2 + x_2^2 - 1$, $f(\mathbf{x}) = -4 + y_d(\mathbf{x})$ and the tracking type cost $j(\mathbf{x}, y(\mathbf{x})) = \frac{1}{2}\left(y(\mathbf{x}) - y_d(\mathbf{x})\right)^2$. We fix $\alpha = 2$ for the non homogeneous Neumann boundary condition. We consider the case $E = \emptyset$, $J = 0$ and $L = 0$, with the numerical parameters: $\epsilon = 0.5$, the mesh of D has 73786 triangles and 37254 vertices. Here, in the cases a) and b), at each line-search, we evaluate 30 times the cost function.

The initial domain is the disk of center $(0, 0)$ and radius 2.5 with a circular hole of center $(-1, -1)$ and radius 0.5. The corresponding $g_0(x_1, x_2)$ is given by

$$\max\left((x_1)^2 + (x_2)^2 - 2.5^2, -(x_1+1)^2 - (x_2+1)^2 + 0.5^2\right).$$

The initial guess for the control is $u_0 = 0$. These ad hoc initial choices are obtained after several attempts. Some intuition in this respect may be offered by the maximum principle in the elliptic system. The guess $u_0 = 0$ simplifies the approximating system, for $k = 0$. In "real life" problems, the initial iteration should be inspired by the physical configuration that has to be improved.

We use here the direction given by the Proposition 5.2, part ii) and the algorithm stops after 3 iterations, when no new descent direction is found in this simplified setting.

We can observe in Figure 2 the evolution of the domain (both boundary and topological changes) and in Table 3 the corresponding values of the objective function. For $u_0 = 0$, we get $g_1 = g_0$ (the same geometry), but we have a strictly lower value for the cost functional, since there is minimization with respect to the control u. Numerically, we solve just the control problem, according to Proposition 5.2, and we compute in each step k, the variations $[g_h, u_h]+\lambda[r_h, v_h]$. According to the values of λ, the topology (given by $g_h + \lambda r_h$) may change as explained in Rem. 5.4.

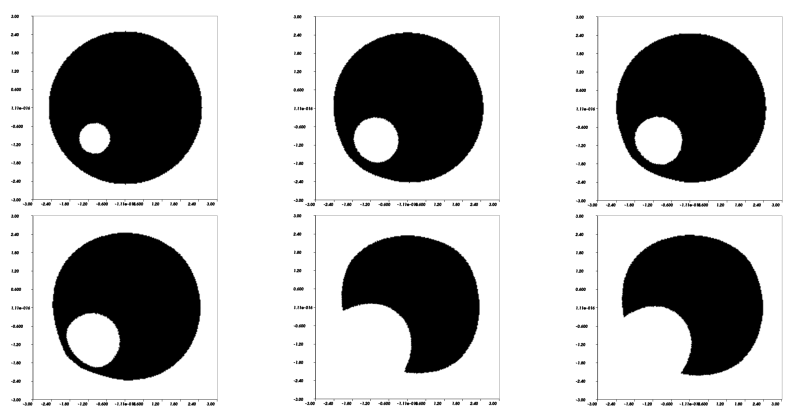

Figure 2: Example 2, case a). Initial domain $k = 0$ and domain for $k = 1$ (top, left), some intermediate domains during the line-search after $k = 1$ ($i = 14$, top, middle) ($i = 13$, top, right), ($i = 11$, bottom, left), ($i = 6$, bottom, middle) and the final domain $k = 2$ (bottom, right). At each line-search, we evaluate the cost function as in Example 1, for $\lambda = \beta^i$, $i = 0, \ldots, 29$, but we plot only some of them, where topology changes.

it.	k=0	k=1				k=2
t_2	220.874	171.135	154.923	149.9	134.41	57.4265	67.7218
t_3	35.5081	34.6306	39.7375	39.0612	35.3332	34.0982	15.7997
$\mathcal{J}$	291.891	240.396	234.398	228.022	205.077	125.623	99.3212

Table 3: Example 2, case a). The computed objective function $\mathcal{J} = t_2 + \frac{1}{\epsilon} t_3$. The columns 4, 5, 6, 7 correspond to some intermediate configurations obtained during the line-search after $k = 1$, the same as in Figure 2. For $k = 0$ and $k = 1$ the domains are identical but the cost function are different. The descent property is valid just for the total cost.

For the solution of the original elliptic problem (2.1)-(2.2) in the computed domains Ω_g, we obtain in fact the best value $t_2 = 53.49$ (see Table 4). This is due to the penalization term t_3, that remains "far" from zero in this experiment. The solution of (2.1)-(2.2) is different from its approximation computed in D. Such situations are frequent in penalization numerical approaches for nonconvex minimization problems.

it.	k=0 and k=1					k=2
t_2	96.3978	76.064	74.4721	87.8033	53.4914	57.6818

Table 4: Example 2, case a). The values of t_2 for the finite element solution of (2.1), (2.2) in the domains obtained in Figure 2.

Case b). We indicate now a variant using the Proposition 5.2, part iii) combined with the descent direction method with projection, see [14]. We study a case with $E \neq \emptyset$ and we choose as before $D =]-3,3[\times]-3,3[$, $y_d(x_1,x_2) = x_1^2 + x_2^2 - 1$, $f(\mathbf{x}) = -4 + y_d(\mathbf{x})$ and $\alpha = 2$. The observation domain E is the disk of center $(0,0)$ and radius 0.5 and we take $J(\mathbf{x}, y(\mathbf{x})) = \frac{1}{2}\left(y(\mathbf{x}) - y_d(\mathbf{x})\right)^2$, $j = 0$ and $L = 0$. We fix $\epsilon = 0.9$ and the mesh of D has 73786 triangles and 37254 vertices. For $g_0(x_1,x_2)$, given by

$$\max\left((x_1+0.8)^2 + (x_2+0.8)^2 - 1.8^2, -(x_1+0.8)^2 - (x_2+0.8)^2 + 0.6^2\right)$$

the initial domain is the ring of center $(-0.8,-0.8)$, exterior radius 1.8 and interior radius 0.6. The initial guess for the control is $u_0 = 1$.

In order to observe during the algorithm the restriction (2.5), the projection is computed as follows: $\Pi(g) = g_E$ in E and $\Pi(g) = g$ outside E, where $g_E \in \mathcal{F}$ is such that $g_E(\mathbf{x}) < 0$ if and only if $\mathbf{x} \in E$. In our test, $g_E(x_1, x_2) = (x_1)^2 + (x_2)^2 - 0.5^2$. The line search, using projection only for the parametrization function associated to the geometry, is

$$\lambda_k \in \arg\min_{\lambda > 0} \mathcal{J}\left(\Pi(G^k + \lambda R^k), U^k + \lambda V^k\right)$$

and the next iteration is defined by

$$G^{k+1} = \Pi(G^k + \lambda_k R^k), \quad U^{k+1} = U^k + \lambda_k V^k.$$

The algorithm stops after two iterations, when no new descent direction is found in this simplified setting. The domain evolution includes topological and boundary changes and is presented in Figure 3. The corresponding values of the objective function are given in Table 5.

For the finite element solution of the original state system (2.1)-(2.2) in the domains presented in Figure 3, we have reported t_1 in Table 6. Due to the low value of the initial cost, we notice the oscillations around this value and the minimal cost is attained already in the first step of the line search. The interpretation of the values of the penalization term is similar as in the previous case a).

it.	k=0				k=1	k=2
t_1	8.03257	6.01812	4.00209	3.37499	0.356422	0.549549
t_3	234.917	218.348	204.479	198.083	193.56	57.4223
$\mathcal{J}$	269.052	248.627	231.2	223.467	215.423	64.3521

Table 5: Example 2, case b). The computed objective function $\mathcal{J} = t_1 + \frac{1}{\epsilon} t_3$. The columns 3, 4, 5 correspond to some intermediate configurations obtained during the line-search after $k = 0$, the same as in Figure 3.

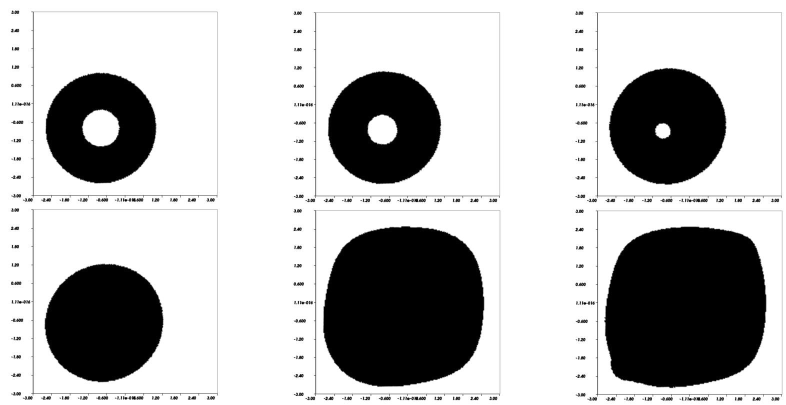

Figure 3: Example 2, case b). Domain for $k=0$ (top, left), some intermediate domains during the line-search after $k=0$, ($i=17$, top, middle), ($i=13$, top, right), ($i=12$, bottom, left), domain for $k=1$ (bottom, middle) and the final domain for $k=2$ (bottom, right). At each line-search, we evaluate 30 times the cost function as in Example 1.

it.	k=0				k=1	k=2
t_1	0.0999952	0.000530429	0.118303	0.272773	0.518959	0.498004

Table 6: Example 2, case b). The values of t_1 for the finite element solution of (2.1), (2.2) in the domains presented in Figure 3.

Example 3.

Case a). We use here the descent direction given by the Corollary 5.1. We fix $D =]-3,3[\times]-3,3[$, $y_d(x_1,x_2) = x_1^2 + x_2^2 - 1$, $f(\mathbf{x}) = -4 + y_d(\mathbf{x})$, $\alpha = 2$, $\epsilon = 0.05$ and we work with $J = 0$, $j(\mathbf{x}, y(\mathbf{x})) = -\frac{1}{2}\left(y(\mathbf{x}) - y_d(\mathbf{x})\right)^2$, $L = 0$. The initial domain is given by

$$g_0(x_1,x_2) = \max\left(x_1^2 + x_2^2 - 0.9^2, -(x_1+0.5)^2 - (x_2+0.5)^2 + 0.5^2\right)$$

and the initial guess for the control is $u_0 = 0$. The mesh of D has 78580 triangles and 39651 vertices. In the case a), at each line-search, we evaluate 60 times the cost function, by choosing $\lambda = \beta^i$ as previously. For the case b), we use Armijo rule, [10]. The algorithm stops after $k = 4$ iterations.

In Figure 4 and Table 7 we present the domain evolution and the corre-

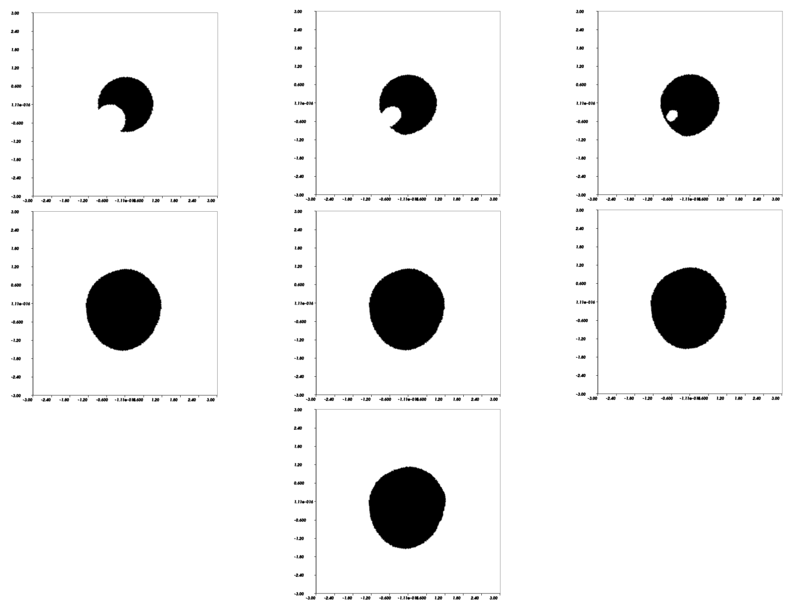

Figure 4: Example 3, case a). Top: domain for $k = 0$ (top, left), some intermediate domains during the line-search after $k = 0$ ($i = 12$, top, middle), ($i = 10$, top, right); middle: domains for $k = 1$, $k = 2$, $k = 3$; bottom: domain $k = 4$ (final).

sponding values of the objective function. We show in Table 8 the values of t_2 for the finite element solution of (2.1), (2.2) and in Table 11 the relative error of the objective function.

This example shows that the main algorithm performs well in general situations (for instance, here $j(\cdot,\cdot)$ is not positive) and may generate new holes during the iterations. The descent property is also clear in Table 7. However, in Table 8 this does not remain valid, in passing from $k = 0$ to $k = 1$. The assumption $j(\cdot,\cdot)$ positive of Prop. 3.1, Prop. 3.2 is not satisfied here.

it.	k=0			k=1	k=2	k=3	k=4
t_2	-10.6838	-12.6079	-13.777	-21.6806	-21.3413	-21.0212	-21.4145
t_3	11.6691	11.5843	11.0201	4.06012	3.94102	3.84741	3.81699
$\mathcal{J}$	222.698	219.077	206.625	59.5217	57.479	55.9271	54.9253

Table 7: Example 3, case a). The computed objective function $\mathcal{J} = t_2 + \frac{1}{\epsilon} t_3$. The columns 3 and 4 are for some intermediate domains during the line-search after $k = 0$, the same as in Figure 4.

it.	k=0			k=1	k=2	k=3	k=4
t_2	-16.7263	-8.64467	-4.98316	-4.2389	-4.25436	-4.26671	-4.54276

Table 8: Example 3, case a). The values of t_2 for the finite element solution of (2.1), (2.2). The columns 3 and 4 are for some intermediate domains during the line-search after $k = 0$, the same as in Figure 4.

Case b). We have pointed out, before the Proposition 3.1, that one may also use homogeneous Neumann boundary conditions on ∂D, instead of homogeneous Dirichlet boundary conditions. It is just necessary to operate this change in (3.3) for y and in (4.2) for q. At the discrete level, we replace $\mathbb{V}_h$ by $\mathbb{W}_h$ in (5.14), (5.15), etc, in order to work with $y_h, q_h, p_h \in \mathbb{W}_h$, as well as the test function $\varphi_h \in \mathbb{W}_h$. All the theoretical arguments remain valid.

We keep the framework of the Example 3, case a), but we use $j(\mathbf{x}, y(\mathbf{x})) = \frac{1}{2}\left(y(\mathbf{x}) - y_d(\mathbf{x})\right)^2$.

At the line-search, we solve

$$\min_{\lambda=\beta^i} \mathcal{J}\left((G^k, U^k) + \lambda(R^k, V^k)\right)$$

with $\beta = 0.8$. In addition, we used at the line-search the Armijo rule to get the first $i = 0, 1, \ldots$ such that

$$\mathcal{J}\left((G^k, U^k) + \beta^i (R^k, V^k)\right) < \mathcal{J}\left(G^k, U^k\right) + \sigma\beta^i \, d\mathcal{J}_{(G^k,U^k)}(R^k, V^k)$$

with $\sigma = 10^{-9}$ and $\beta = 0.8$, see for example [10], p. 29. The algorithm stops after $k = 4$ iterations. The numerical results are presented in Figure 5 and Tables 9, 10, 11.

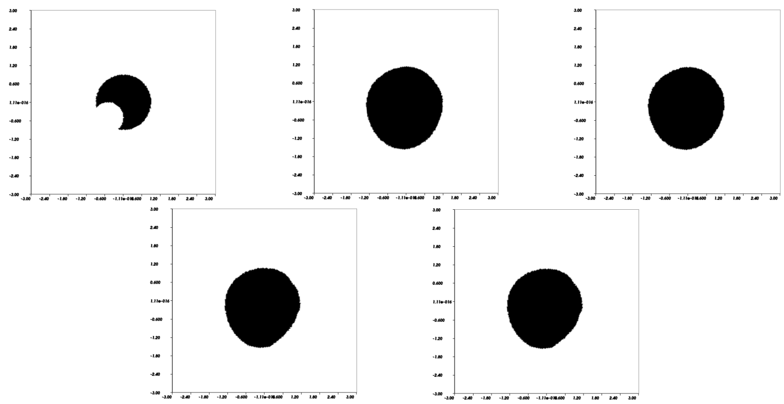

Figure 5: Example 3, case b) Armijo rule. Top: domain for $k = 0$ (left), $k = 1$, $k = 2$; bottom: $k = 3$, $k = 4$ (final).

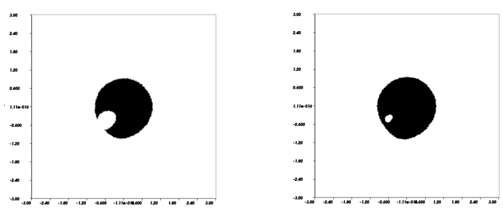

Figure 6: Example 3, case b) Armijo rule. Domain transformations after $k = 0$ for $i = 13$ (left) and $i = 11$ (right).

The Armijo rule allows to reduce the number of the evaluations of the objective function at each line-search: 2 evaluations at $k = 0$; 1 evaluation at $k = 1$ and $k = 2$; 19 evaluations at $k = 3$.

At the initial step $k = 0$, the two evaluations correspond to $i = 0$ and $i = 1$, that is to $\lambda = 1$, respectively $\lambda = 0.8$ that yields the iteration $k = 1$. The evolution of the geometry between these two steps includes topological transformations. For instance, computing the unknowns for $i = 13$ and $i = 11$, one obtains (see Fig. 6).

it.	k=0	k=1	k=2	k=3	k=4
t_2	6.21443	17.7813	13.7137	10.6477	10.7381
t_3	10.3086	4.39795	2.49773	1.58751	1.58084
$\mathcal{J}$	212.386	105.74	63.6683	42.3979	42.3549

Table 9: Example 3, case b) Armijo rule. The computed objective function $\mathcal{J} = t_2 + \frac{1}{\epsilon}t_3$.

it.	k=0	k=1	k=2	k=3	k=4
t_2	16.7263	4.86361	4.77218	3.60206	3.64877

Table 10: Example 3, case b) Armijo rule. The values of t_2 for the finite element solution of (2.1), (2.2).

Our technique has the capacity to generate holes. The obtained objective function $\mathcal{J} = t_2 + \frac{1}{\epsilon}t_3$ has the values 206.834, 147.325 respectively, in these points. The corresponding values of t_2 for the finite element solution of (2.1), (2.2) are 8.70233, 1.71132 respectively. Working in the domain D with the Armijo rule and the penalization technique is very efficient and gives a good local solution. However, the cost associated to the domain with a hole happens to be even lower.

it.	k=0	k=1	k=2	k=3
Ex. 1 a)	0.982098	0.964812	0.666710	0.121442
Ex. 3 a)	0.732724	0.034318	0.026999	0.017912
Ex. 3 b)	0.502132	0.397878	0.334081	0.001014

Table 11: Relative error $\frac{|\mathcal{J}(G^{k+1},U^{k+1}) - \mathcal{J}(G^k,U^k)|}{|\mathcal{J}(G^k,U^k)|}$ in Example 1 a) and Example 3 a) b).

Acknowledgement We thank the anonymous referees for the very helpful suggestions and remarks that improved the presentation.

References

[1] G. Allaire, Conception optimale de structures, Volume 58 of Mathématiques & Applications [Mathematics & Applications]. Springer-Verlag, Berlin, 2007.

[2] G. Allaire, F. Jouve, A-M. Toader, A level-set method for shape optimization. C. R. Math. Acad. Sci. Paris, 334 (2002), no. 12, 1125–1130.

[3] S. Amstutz, The topological asymptotic for the Navier-Stokes equations. ESAIM Control Optim. Calc. Var. 11 (2005), no. 3, 401–425.

[4] S. Amstutz, H. Andra, A new algorithm for topology optimization using a level-set method. J. Comput. Phys. 216 (2006), no. 2, 573–588.

[5] S. Amstutz, A. Bonnafé, Topological derivatives for a class of quasilinear elliptic equations. Journal de Mathématiques Pures et Appliquées, 107 (2017), no. 4, 367–408.

[6] S. Amstutz, M. Masmoudi, B. Samet, The topological asymptotic for the Helmholtz equation, SIAM J. Control Optim. 42 (2003), no. 5, 1523–1544.

[7] V. Arnautu, H. Langmach, J. Sprekels, D. Tiba, On the approximation and optimization of plates, Numer. Funct. Anal. Optim. 21 (2000) no. 3-4, 337–354.

[8] M. Barboteu, M. Sofonea, D. Tiba, The control variational method for beams in contact with deformable obstacles, Z. Angew. Math. Mech. 92, (2012) no. 1, 25–40.

[9] M. P. Bendsoe, O. Sigmund, Topology Optimization: Theory, Methods, and Applications, second edition, Springer-Verlag, Berlin, 2003.

[10] D. Bertsekas, Nonlinear Programming, second edition, Athena Scientific, 1999.

[11] D. Bucur, G. Buttazzo, Variational methods in shape optimization problems, Progress in Nonlinear Differential Equations and their Applications, 65. Birkhauser Boston, Inc., Boston, MA, 2005.

[12] M. Burger, A framework for the construction of level set methods for shape optimization and reconstruction, Interfaces Free Bound. 5 (2003), 301–329.

[13] P. G. Ciarlet, The finite element method for elliptic problems. Classics in Applied Mathematics, 40. Society for Industrial and Applied Mathematics (SIAM), Philadelphia, PA, 2002.

[14] P. G. Ciarlet, Introduction to Numerical Linear Algebra and Optimization, Cambridge University Press, 2018.

[15] C. Clason, K. Kunisch, A convex analysis approach to multi-material topology optimization, ESAIM Math. Model. Numer. Anal. 50 (2016), no. 6, 1917–1936.

[16] C. Clason, F. Kruse, K. Kunisch, Total variation regularization of multi-material topology optimization, ESAIM Math. Model. Numer. Anal. 52 (2018), no. 1, 275–303.

[17] M.C. Delfour, J.P. Zolesio, Shapes and Geometries, Analysis, Differential Calculus and Optimization, SIAM, Philadelphia, 2001.

[18] P. Gangl, K. Sturm, A simplified derivation technique of topological derivatives for quasi-linear transmission problems, ESAIM Control Optim. Calc. Var., 26 (2020), 106.

[19] P. Grisvard, Elliptic Problems in Nonsmooth Domains. London, Pitman, 1985.

[20] A. Halanay, C.M. Murea, D. Tiba, Existence of a steady flow of Stokes fluid past a linear elastic structure using fictitious domain, J. Math. Fluid Mech. 18 (2016), no. 2, 397–413.

[21] A. Halanay, C.M. Murea, D. Tiba, Extension theorems related to a fluid-structure interaction problem, Bull. Math. Soc. Sci. Math. Roumanie, 61 (2018) 417–437.

[22] J. Haslinger, P. Neittaanmäki, Finite element approximation of optimal shape design, J. Wiley & Sons, New York, 1996.

[23] M. Hassine, S. Jan, M. Masmoudi, From differential calculus to 0-1 topological optimization. SIAM J. Control Optim. 45 (2007), no. 6, 1965–1987.

[24] F. Hecht, New development in FreeFem++. J. Numer. Math. 20 (2012) 251–265. http://www.freefem.org

[25] A. Henrot, M. Pierre, Variations et optimisation de formes. Une analyse géométrique, Springer, 2005.

[26] M.W. Hirsch, S. Smale, L.R. Devaney, Differential Equations, Dynamical Systems and an Introduction to Chaos, Elsevier, Academic Press, San Diego, 2014.

[27] R. Mäkinen, P. Neittaanmäki, D. Tiba, On a fixed domain approach for a shape optimization problem, in: Computational and applied Mathematics II: Differential equations (W.F. Ames, P.J. van Houwen, eds.), North Holland, Amsterdam, 1992, pp. 317–326.

[28] A. Maury, G. Allaire, F. Jouve, Shape optimization with the level set method for contact problems in linearised elasticity, SMAI Journal of Computational Mathematics, 3 (2017), 249–292.

[29] C.M. Murea, D. Tiba, Topological optimization via cost penalization, Topological Methods in Nonlinear Analysis, 54 (2019), No. 2B, 1023–1050.

[30] C.M. Murea, D. Tiba, Optimization of a plate with holes, Computers and Mathematics with Applications, 77 (2019) 3010–3020.

[31] P. Neittaanmäki, D. Tiba, Fixed domain approaches in shape optimization problems, Inverse Problems, 28 (2012) 1–35.

[32] P. Neittaanmäki, A. Pennanen, D. Tiba, Fixed domain approaches in shape optimization problems with Dirichlet boundary conditions, Inverse Problems, 25 (2009) 1–18.

[33] P. Neittaanmäki, J. Sprekels, D. Tiba, Optimization of elliptic systems. Theory and applications, Springer, New York, 2006.

[34] M.R. Nicolai, D. Tiba, Implicit functions and parametrizations in dimension three: generalized solutions. Discrete Contin. Dyn. Syst. 35 (2015), no. 6, 2701–2710.

[35] A. Novotny, J. Sokolowski, Topological derivatives in shape optimization, Springer, Berlin, 2013.

[36] A. Novotny, J. Sokolowski, A, Zochowski, Applications of the Topological Derivative Method, Springer Studies in Systems, Decision and Control 188, 2019.

[37] S. Osher, R. Fedkiw, Level set methods and dynamic implicit surfaces, Volume 153 of Applied Mathematical Sciences. Springer-Verlag, New York, 2003.

[38] S. Osher, J.A. Sethian, Fronts propagating with curvature-dependent speed: algorithms based on Hamilton-Jacobi formulations. J. Comput. Phys. 79 (1988), no. 1, 12–49.

[39] O. Pironneau, Optimal shape design for elliptic systems, Springer, Berlin, 1984.

[40] L.S. Pontryagin, Equations Differentielles Ordinaires, MIR, Moscow, 1968

[41] A. Quarteroni, R. Sacco, F. Saleri, Numerical mathematics. Second edition. Texts in Applied Mathematics, 37. Springer-Verlag, Berlin, 2007.

[42] P.-A. Raviart and J.-M. Thomas, Introduction à l'analyse numérique des équations aux dérivées partielles. Dunod, 2004.

[43] J. Sokolowski, J.P. Zolesio, Introduction to Shape Optimization. Shape Sensitivity Analysis, Springer, Berlin, 1992.

[44] D. Tiba, A property of Sobolev spaces and existence in optimal design. Appl. Math. Optim. 47 (2003), no. 1, 45–58.

[45] D. Tiba, The implicit function theorem and implicit parametrizations. Ann. Acad. Rom. Sci. Ser. Math. Appl. 5 (2013), no. 1-2, 193–208.

[46] D. Tiba, Iterated Hamiltonian type systems and applications. J. Differential Equations, 264 (2018), no. 8, 5465–5479.

[47] D. Tiba, A penalization approach in shape optimization, Atti della Accademia Peloritana dei Pericolanti - Classe di Scienze Fisiche, Matematiche e Naturali, 96 (2018), no. 1, A8.

[48] D. Tiba, Implicit parametrizations and applications in optimization and control, Mathematical Control and Related Fields, 10 (2020), no. 3, 455–470.

[49] D. Tiba, M. Yamamoto, A parabolic shape optimization problem, Ann. Acad. Rom. Sci. Ser. Math. Appl. 12 (2020), no. 1-2, 312–328.

[50] S.Y. Wang, M.Y. Wang, Structural Shape and Topology Optimization Using an Implicit Free Boundary Parametrization Method, Computer Modeling in Engineering and Sciences, 13 (2006), no. 2, 119–147.

[51] Wikipedia, the free encyclopedia, `https://en.wikipedia.org/wiki/Riemann_sum`